Supplemental Material to: 'Dry Active Matter exhibits a self-organized "Cross Sea" Phase'

Rüdiger Kürsten and Thomas Ihle

Institut für Physik, Universität Greifswald, Felix-Hausdorff-Str. 6, 17489 Greifswald, Germany

September 17, 2020

1 Lattice Order Parameter

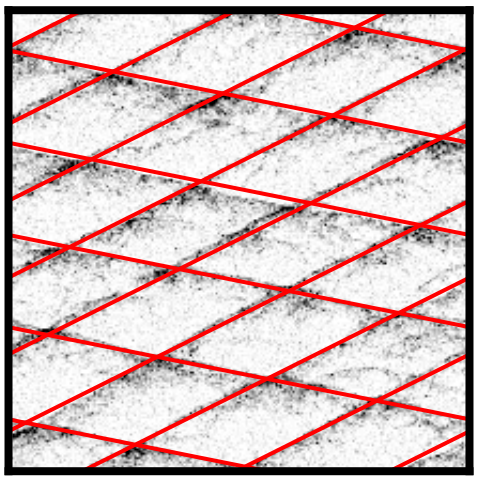

Figure S1: Snapshot of Fig. 1 (*ii*) of the Letter together with the wave fronts (red lines) of the wave vectors $\mathbf{k}_1$ and $\mathbf{k}_2$ that have the largest amplitudes in the Fourier transform of the density.

In the cross sea phase, the particle density is significantly higher at the crossing points of the pattern compared to the density at patterns fronts away from the crossing points, see Fig. 4 of the Letter. Those high density regions form a regular Bravais lattice in two dimensions. For a perfect Bravais lattice the reciprocal lattice is given by a Fourier transform of the density. We perform a Fourier transform of the local particle density of the cross sea state

$$\hat{f}_{\mathbf{k}} := \frac{1}{N}\sum_{j=1}^{N} \exp(i\mathbf{k}\cdot\mathbf{r}_j), \tag{S.1}$$

where $\mathbf{k} = \frac{2\pi}{L}\binom{n_x}{n_y}$ with integers n_x and n_y. We exclude the case $n_x = n_y = 0$ because the result is trivially equal to one and the case $n_x < 0$ because $\hat{f}_{\mathbf{k}} = \hat{f}^*_{-\mathbf{k}}$, where * denotes complex conjugation. Looking for the two $\mathbf{k}$-vectors $\mathbf{k}_1$ and $\mathbf{k}_2$ with amplitudes that have the highest absolute value, we find indeed the $\mathbf{k}$-vectors that describe the pattern. In Fig. S1 we show the snapshot of Fig. 1 (ii) of the Letter from the cross sea phase with additional the red lines indicating the wave fronts corresponding to $\mathbf{k}_1$ and $\mathbf{k}_2$.

It is reasonable to use the geometric mean of $|\hat{f}_{\mathbf{k}_1}|$ and $|\hat{f}_{\mathbf{k}_2}|$, that is

$$l = \sqrt{|\hat{f}_{\mathbf{k}_1}| \cdot |\hat{f}_{\mathbf{k}_2}|} \tag{S.2}$$

as lattice order parameter. If the particles were arranged in a perfect Bravais lattice, that is if the particles were equally distributed over all lattice sites, the resulting lattice order parameter would be $l = 1$. For the example of Fig. S1 we obtain $l \approx 0.32$. In the Toner-Tu phase and in the disordered phase we expect that $l = 0$. For the examples of Figs. 1 (i) and (iv) of the lattice we find values of $l \approx 0.064$ and $l \approx 0.009$, respectively, which is at least significantly smaller than in the cross sea phase. The band phase (iii) has only one characteristic wave vector, and indeed, we find that $\mathbf{k}_2 = 2\mathbf{k}_1$ in most cases in the band phase. That leads to values of l which are comparable to the cross sea phase. Therefore, to distinguish between cross sea and band phase, we forbid multiples of $\mathbf{k}_1$ in the definition of $\mathbf{k}_2$. That means $\mathbf{k}_1$ is the wave vector with largest amplitude and $\mathbf{k}_2$ is the wave vector with largest amplitude from the remaining vectors that are not multiples of $\mathbf{k}_1$.

In Fig. S2 (a) we display the average value of the lattice order parameter. Its qualitative behavior is completely equivalent to the structural order parameter C_2. In the Toner-Tu phase we find a value of roughly $l \approx 0.05$ in the cross sea phase $l \approx 0.3$, in the band phase $l \approx 0.2$ and in the disordered phase $l \approx 0$. The Binder cumulant of the lattice order parameter is shown in Fig. S2 (b). It has local minima almost at the same positions as the Binder cumulant of C_2. We find only a small deviation for the transition between Toner-Tu (i) and cross sea phase (ii), where the minimum of $B(C_2)$ is at $\eta = 0.284$ and the minimum of $B(l)$ is at $\eta = 0.280$. However the difference of $B(C_2)$ between the two points is almost zero. We conclude that the lattice order parameter l can equally well be used to study the transition of the Vicsek model. Its equivalent behavior compared to the C_2 order parameter confirms the existence of cross sea states as a distinguished phase.

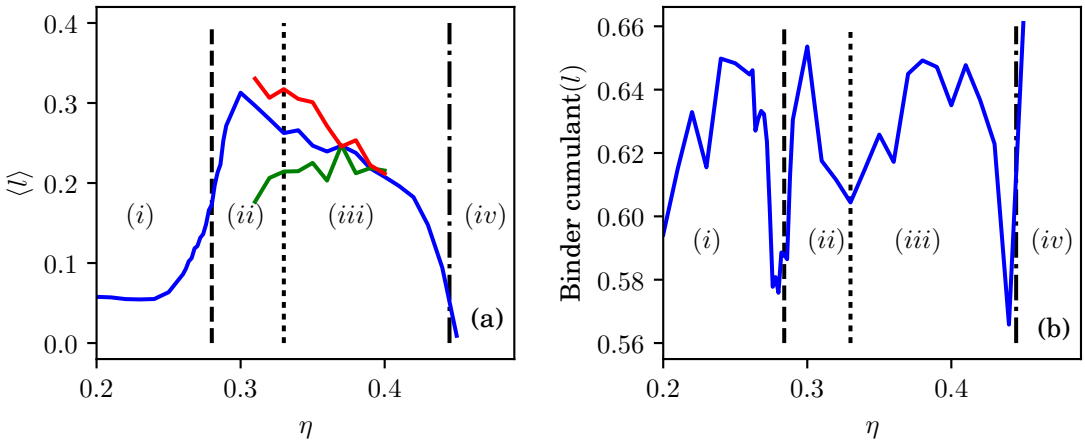

Figure S2: Average value (a) and Binder cumulant (b) of the lattice order parameter l defined in Eq. (S.2) for the same realizations (and parameters) as used in Fig. 2 of the Letter. We used a thermalization time of 10^5 time steps and calculated the order parameter l every 100 time steps, collecting 100 data points for each realization to estimate the moments of l. The red and green line in (a) correspond to the average of realizations that are in the cross sea or band phase, respectively, analogous to Fig. 2 of the Letter. The vertical lines show the transition noise strength η_{c1}, η_{c2} and η_{c3} that are given in the Letter.

1.1 Distribution of Crossing Angles

The crossing angle of the fronts within the cross sea pattern is given by the angle between the wave vectors $\mathbf{k}_1$ and $\mathbf{k}_2$. In Fig. S3 (black circles, blue line) we show the distribution of the crossing angle in the cross sea phase ($\eta = 0.29$) on a quadratic simulation domain. We find a major peak, centered slightly below $\alpha = \pi/4$. Due to boundary effects there is a coupling between the direction of the average velocity and allowed wave vectors. This effect might cause a broadening of the distribution of crossing angles. We expect that those boundary effects decrease and that the peak is narrowed for larger system sizes. The small peak close to zero is caused by four realizations that are still not in steady state, see Fig. S4. They look similar to cross sea states but they are still not a perfect regular pattern. This results in wave vectors with a very small crossing angle. For an aspect ratio of the simulation domain of $1 : 4$ we find the peak located at the same position, see green crosses in Fig. S3 (these data are fluctuating a little more because we used only 15 realizations). We conclude that the picking of crossing angles is self-organized and not a boundary effect. This inherent selection of a crossing angle is another proof showing that the pattern is self-organized and not just a superposition of two waves.

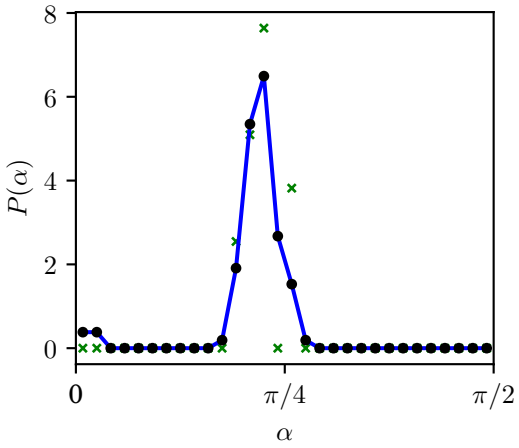

Figure S3: Distribution of the crossing angle of the cross sea pattern sampled over 100 realizations at $\eta = 0.29$ on a quadratic simulation domain (black circles, blue line as a guide to the eyes) and sampled over 15 realizations on a simulation domain with aspect ratio $1:4$ (green crosses). Other parameters are as in the Letter.

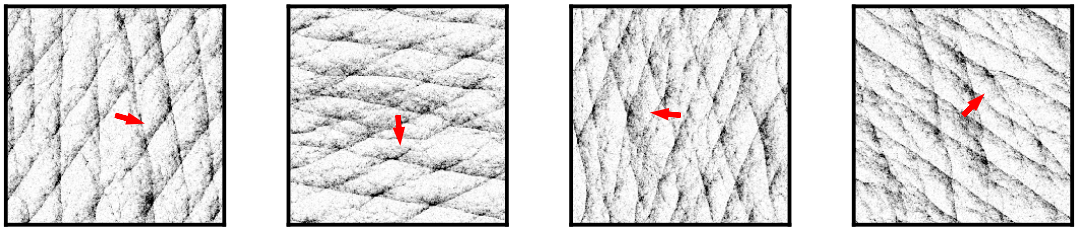

Figure S4: Snapshots of four (of 100) realizations that are not in steady after 2×10^5 time steps. These realizations cause the small peak close to zero in Fig. S3.

1.2 Wave Length of Cross Sea and Band Patterns

We can calculate the wavelength $\lambda = 2\pi/|\mathbf{k}_1|$ of the mode with largest amplitude for cross sea states and for band states, see Fig. S5. We find that this wavelength is larger by a factor of ≈ 2 for cross sea states compared to band states showing the discontinuous nature of the transition. Furthermore, this implies that larger systems are necessary to observe cross sea states, see also Sec. 7.3.

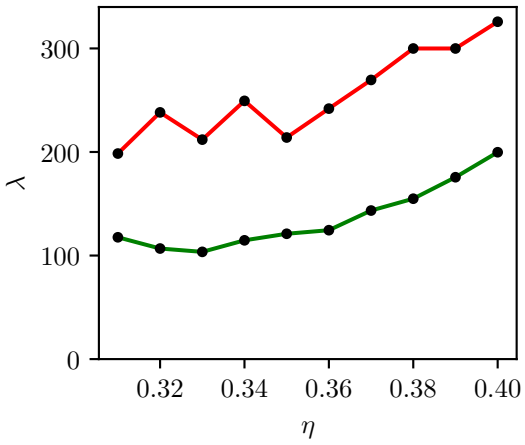

Figure S5: Wavelength $\lambda = 2\pi/|\mathbf{k}_1|$ corresponding to the largest amplitude Fourier mode of the particle density averaged over cross sea states (red line) and band states (green line). Parameters are as in the Letter.

2 Polar Order Parameter

One might want to study the transitions of the Vicsek model considering only the polar order parameter $p := 1/N|\sum_i \mathbf{v}_i|$. However, unfortunately there is only a very small difference (about 5%) between the polar order parameter of band states and of cross sea states at the same noise strength, see Fig. S6. Furthermore, we observe no jump of the polar order parameter at the transition towards the Toner-Tu phase. Thus, the polar order parameter seems to be useful only in the study of the transition between disorder and band phase. We show its Binder cumulant in Fig. S7. There, we clearly observe the transition between phases (*iv*) and (*iii*), however, not the other transitions. This is reasonable because the polar order parameter of the other phases is almost the same (for the same parameters) as discussed above.

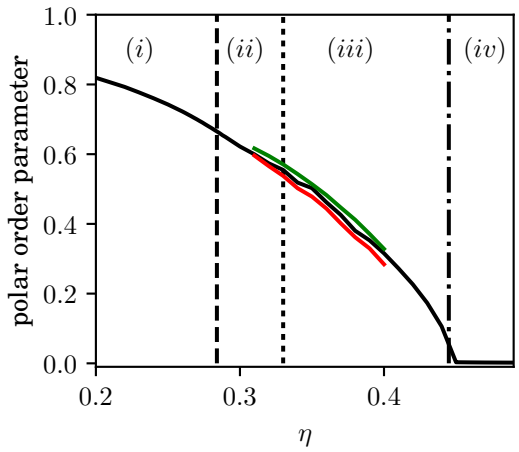

Figure S6: Polar order parameter p averaged over all realizations (black line), only band realizations (green line) and only cross sea realizations (red line) as a function of the noise strength η. Parameters as in Fig. 2 of the Letter.

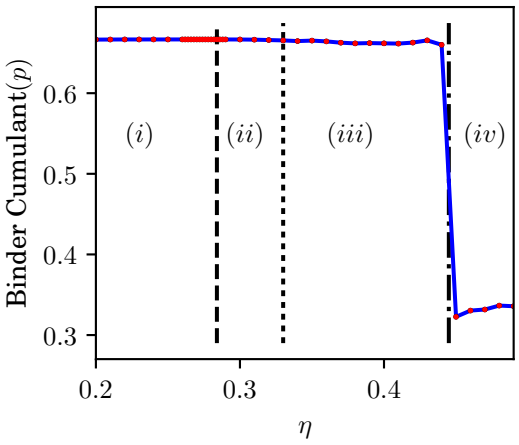

Figure S7: Binder cumulant of the polar order parameter as a function of the noise strength η. It shows the transition between disorder (*iv*) and band phase (*iii*). At this transition, we expect to see an even deeper dip with a higher resolution in η. Parameters as in Fig. 2 of the Letter.

3 Binder Cumulant of C_2

In Fig. 3 of the Letter we show the Binder cumulant of the C_2 order parameter $B(C_2) := 1 - \frac{\langle C_2^4 \rangle}{3\langle C_2^2 \rangle^2}$ where the average $\langle \cdot \rangle$ is performed over different realizations and a time of 10^4 time steps for each realization. The Binder cumulant has local minima between the Toner-Tu phase (*i*) and the cross sea phase (*ii*) and between the cross sea phase and the phase of polar ordered bands (*iii*). Those minima have relatively large values, in particular

for the transition between (i) and (ii). However, the minimum value of the Binder cumulant is known from the theory of first order phase transitions [33]. At the transition point of such a discontinuous transition we expect the probability distribution of the order parameter (sampled from many realizations) to be double-peaked. If the two peaks are located at positions e_1 and e_2, the minimum value of the Binder cumulant is in leading order

$$B_{\min} = \frac{2}{3} - \left(\frac{e_1}{e_2} - \frac{e_2}{e_1}\right)^2 /12 \tag{S.3}$$

for large system sizes [33]. The next order corrections as a function of the system size L depend on the details of the distribution of the order parameter [33]. For the transition between cross sea phase (ii) and band phase (iii) at $\eta_{c2} \approx 0.33$ we can estimate the values of e_1 and e_2 by averaging C_2 over cross sea realizations, or respectively, over band realizations only. The corresponding values are given by the red (cross sea phase) and green (band phase) lines in Fig. 2 of the Letter. The values are $e_1 \approx 8.32$ for the cross sea phase and $e_2 \approx 6.34$ for the band phase resulting in the minimal value of the Binder cumulant $B_{\min} \approx 0.641$ according to Eq. (S.3). The minimum value we measured (which can be read from Fig. 3 of the Letter) is very close at $B(C_2)_{\min} \approx 0.643$. The small deviation is likely caused by a combination of the following reasons. We sampled the noise strength with a relatively rough resolution of 0.01. Thus the real minimum is somewhere in the interval $\eta_{c2} = 0.33 \pm 0.01$ and hence the minimum value of the Binder cumulant might be slightly smaller. Furthermore there is still a measurement uncertainty in the value of the Binder cumulant that could be decreased (and estimated) with significantly more data. Eventually, there are finite size corrections to Eq. (S.3) of unknown form that are neglected here.

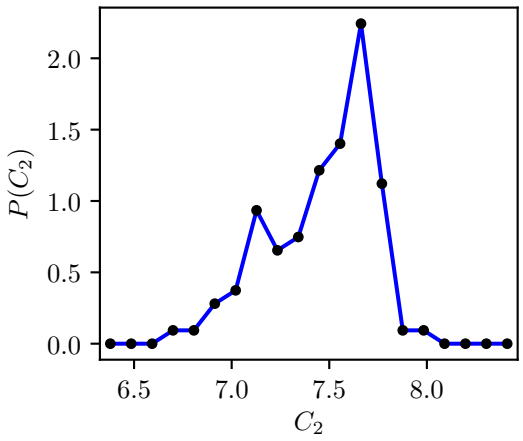

Figure S8: Normalized histogram of the order parameter C_2 at the estimated transition noise strength $\eta_{c1} = 0.284$. The histogram is obtained from 100 realizations. For each data point C_2 was averaged over 10^4 time steps after a thermalization of 2×10^5 time steps. The double peak structure shows the discontinuous nature of the transition. Parameters are as in Fig. 2 of the Letter.

For the transition between (ii) and (iii) it was easy to distinguish the phases (cross sea or bands) by hand. Thus, we could just use the corresponding realizations to obtain the values of e_1 and e_2. For the transition between Toner-Tu phase (i) and cross sea phase (ii) it is not clear how to distinguish the phases by hand. Therefore we made a histogram of the order parameter C_2 over 100 realizations at the estimated transition point $\eta_{c1} = 0.284$, see Fig. S8. Indeed we see a double peak structure of the order parameter. Reading off the local maxima we find the values of $e_1 \approx 7.13 \pm 0.11$ and $e_2 =\approx 7.66 \pm 0.11$ resulting in the minimal value of the Binder cumulant $B_{\min} \approx 0.665 \pm 0.001$. It is consistent with the measured value $B_{\min} \approx 0.6644$.

4 Exact Values of the Transition Points η_{c1} and η_{c2}

To obtain precise estimates of the transition points η_{c1} and η_{c2} finite size scaling is necessary. For that purpose one would need to measure significantly more (and larger) system sizes with a high resolution in η and also more data (more realizations). However, this task is beyond our accessible computational resources (for the numerical results presented in this Letter we used computation times of approximately 10^7 CPU core hours). Furthermore,

in particular for the transition between cross sea phase (*ii*) and band phase (*iii*) it is not clear if the transition point depends on initial conditions (we used random initial conditions, that is, each particles initial position and orientation was drawn independently from a flat distribution). The transition point is reached when the two peaks of the probability distribution of the order parameter have equal weight. This is the case, when half of the realizations are in cross sea states and half of the realizations are in band states. However, this might depend on the initial distribution and the real steady state can be observed only after simulation times that are long enough, such that for each realization, many transitions from cross sea to band and vice versa are observed. In our simulations we observe (at fixed noise intensity) no transitions between cross sea and band states. This is a typical problem in numerical studies of first order phase transitions. It can be avoided by reweighting or flat-histogram sampling techniques. However, to the best of our knowledge, there are no such flat-histogram sampling techniques available that work for non-equilibrium systems of the Vicsek type.

The aim of this work is not to give the precise ($L \to \infty$) transition points η_{c1} and η_{c2}. We restrict ourselves to show that the four phases $(i) - (iv)$ exist and that they are separated by discontinuous transitions.

5 Stationarity of the considered states

It has been mentioned in Ref. [1] that for the band phase of the Vicsek model, the steady state is reached typically after millions of time steps. This is in contrast to thermalization times of 2×10^5 time steps that we used. However, in Ref. [1] no numerical details are given with respect to the relaxation times and it is referred to Ref. [23]. There, relaxation time scales are not explicitly mentioned. One can try to estimate them from movies presented in the supplemental material of Ref. [23]. In the movie 'Sl1_compression_modes.avi' we estimate the time until the steady state is reached as roughly $5 - 7 \times 10^5$ for a system of 2097152 particles in a 2048×2048 simulation box at a noise intensity of $\eta = 0.25$. In another example, shown in the movie 'Sl7_domain-breaking.avi', $N = 1.8 \times 10^5$ particles are simulated on a 100×800 simulation box with noise intensity $\eta = 0.4$. There, however, the system was initially prepared in a special initial state with high density polar ordered particles being distributed over approximately one third of the simulation domain. The interaction radius in all those simulations was $R = 1$ and the velocity is not explicitly given, however, we assume it has the same value $v = 0.5$ as the simulations in the Letter [23]. Thus, for those simulations, the relaxation time towards the steady state seems to be roughly of the order of 10^6 time steps.

For our simulations with the parameter set presented in the Letter, we observe steady states already after 2×10^5 time steps for almost all realizations [1]. One possible reason for the discrepancy might be the larger velocity ($v = 1$) used in our simulations. Furthermore, special initial conditions or channel-like simulation boxes might affect the relaxation times. Additionally, the relaxation time is depending on the parameters, we observe longer relaxation times for an aspect ratio of the simulation domain of $1 : 16$ and for a different parameter set, see Sec. 7. To demonstrate that our simulations are already in steady state after 2×10^5 time steps we compare snapshots of the typical cases after simulation times of 2×10^5 and 2×10^6 time steps. In Fig. S9 Ia and Ib we compare snapshots of the Toner-Tu phase ($\eta = 0.22$). We see no significant change of the system state except for a rotation of the average direction of motion. In Fig. S9 IIa and IIb we see two snapshots of the cross sea phase ($\eta = 0.29$) and no change of the pattern is observable. In Fig. S9 IIIa, IIIb and IVa, IVb we display snapshots at $\eta = 0.32$ for one realization in cross sea state (III) and one realization in the band state (IV). In Fig. S9 Va and Vb we show snapshots in the band phase ($\eta = 0.42$). In all cases, there is no change in the pattern from $T = 2 \times 10^5$ (a) towards $T = 2 \times 10^6$ (b). Simulation parameters are as in the Letter. We also measured the order parameter C_2 for several times in between $T = 2 \times 10^5$ and 2×10^6, see Fig. S10. The order parameter fluctuates a little bit but it is not changing systematically. We conclude that the system configurations are almost in steady state after 2×10^5 time steps.

[1] Considering large numbers of realizations, very few might still not be in steady after the used thermalization times, see snapshots in Sec. 6.

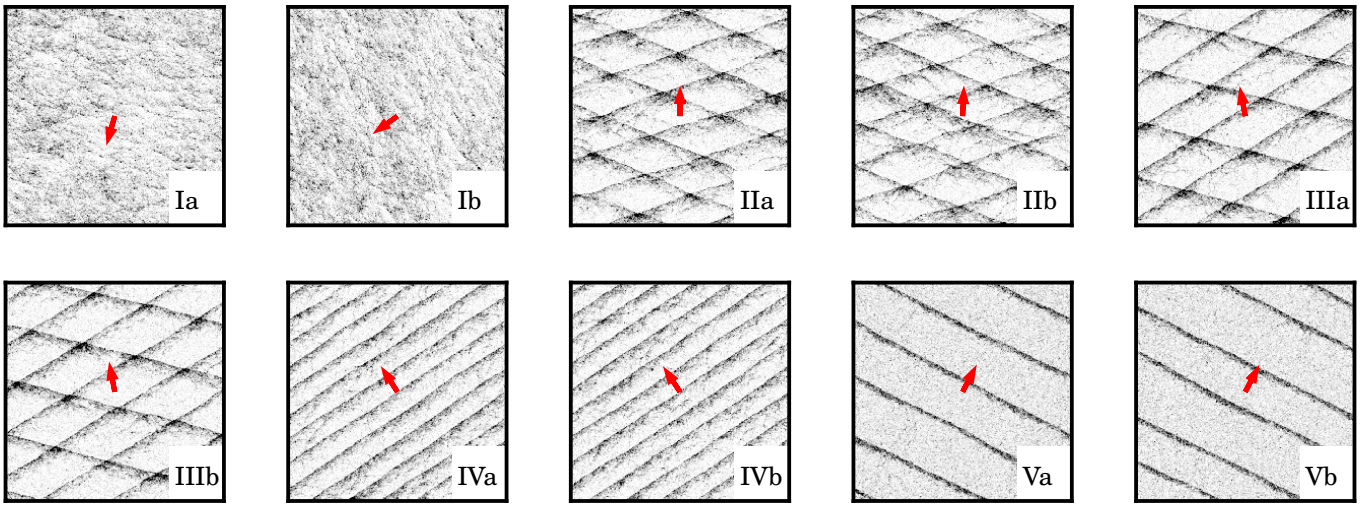

Figure S9: Snapshots for one realization after 2×10^5 (a) and 2×10^6 (b) time steps for noise strength $\eta = 0.22$ (I, Toner-Tu phase), $\eta = 0.29$ (II, cross sea), $\eta = 0.32$ (III, cross sea and IV bands) and $\eta = 0.42$ (V, bands). Other parameters are as in the Letter.

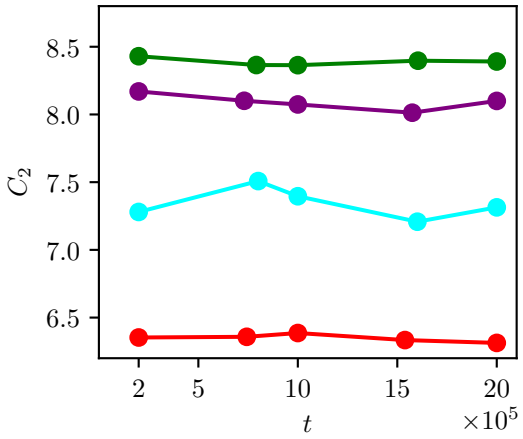

Figure S10: Time dependent structural order parameter C_2 for the cross sea and band realizations shown in Fig. S9: II (purple), III (green), IV (red) and V (cyan). The order parameter was averaged over 10^4 time steps, the time axis represents the first time step of this averaging. We see that the order parameter is fluctuating a little, however, we find no systematic changes which shows that the system is in steady state already after 2×10^5 time steps.

6 Snapshots of the Main Parameter Set

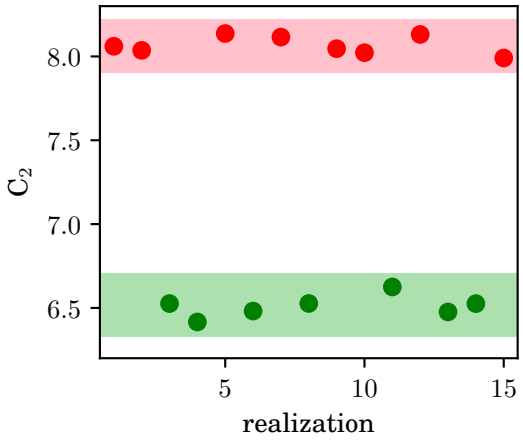

Figure S11: Measured structural order parameter C_2 for 15 realizations for $\eta = 0.36$ and other parameters as in Fig. 2 of the Letter. Red points show realizations that have been classified (by hand) as cross sea states and green points correspond to realizations that have been classified as band states. The values of the order parameter are clearly separated for both phases. Thus one could also use the order parameter to classify the realizations: realizations from the red area are in cross sea and those from the green area are from the band phase.

In this section we present snapshots of the two dimensional standard Vicsek model with parameters: interaction radius $R = 1$, velocity $v = 1$, time step $\Delta t = 1$, particle number $N = 10^6$, system size $L = 1253.3$ for different noise strengths η. This parameter set is the same as the one used in Figs. 2-4 of the Letter. All realizations have been started at random initial conditions and the snapshot was taken after 2×10^5 time steps. The red arrows indicate the average direction of motion.

In the noise range $\eta = 0.31, \ldots, 0.40$ we indicated the cross sea realizations that have been used to calculate the red upper line in Fig. 2 of the Letter by a red frame and the band realizations that have been used to calculate the green lower line by a green frame. The classification as cross sea or band state was done by hand (looking at the snapshot). Alternatively, one can use the structural order parameter C_2 for the classification. We show one example in Fig. S11. We see that the order parameter for realizations from the cross sea phase and from the band phase are clearly separated. Therefore we could also, for that particular parameter set, classify all realizations with $C_2 \in [7.95, 8.20]$ as cross sea and all realizations with $C_2 \in [6.30, 6.60]$ as band states. However, in the Letter we argue that the order parameter has significant different values for realizations in cross sea and in band states, respectively. Classifying the states through the order parameter would be a circular argument. Therefore, we classify the states by hand leading to the same results in any way.

A system configuration similar to the cross sea state has been shown very recently in Fig. 2b of [1]. There, it was described as strongly interacting bands that do not order. In view of the results presented here, we can identify this state as very close to the transition between phases (i) and (ii). It looks very similar to the states we find for $\eta = 0.27$, see below.

$\eta = 0.20$.

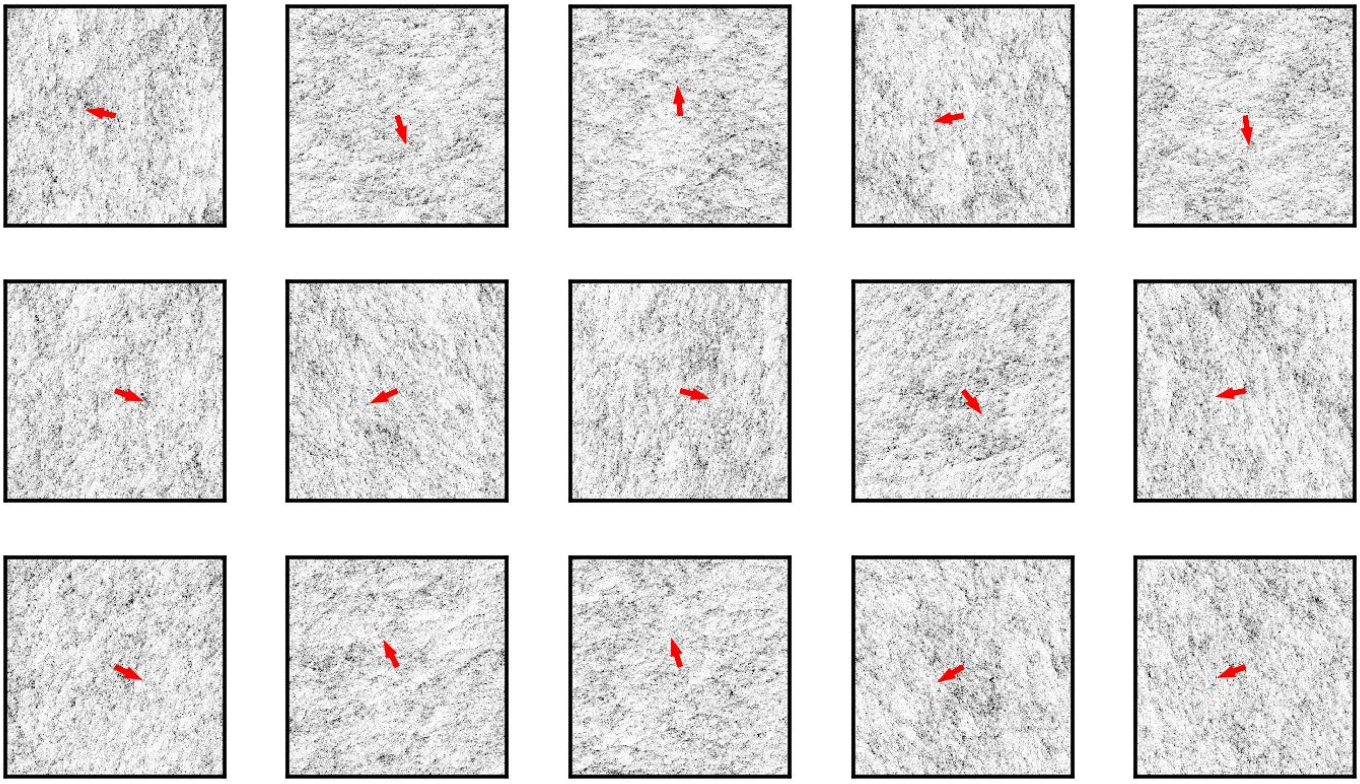

$\eta = 0.21$.

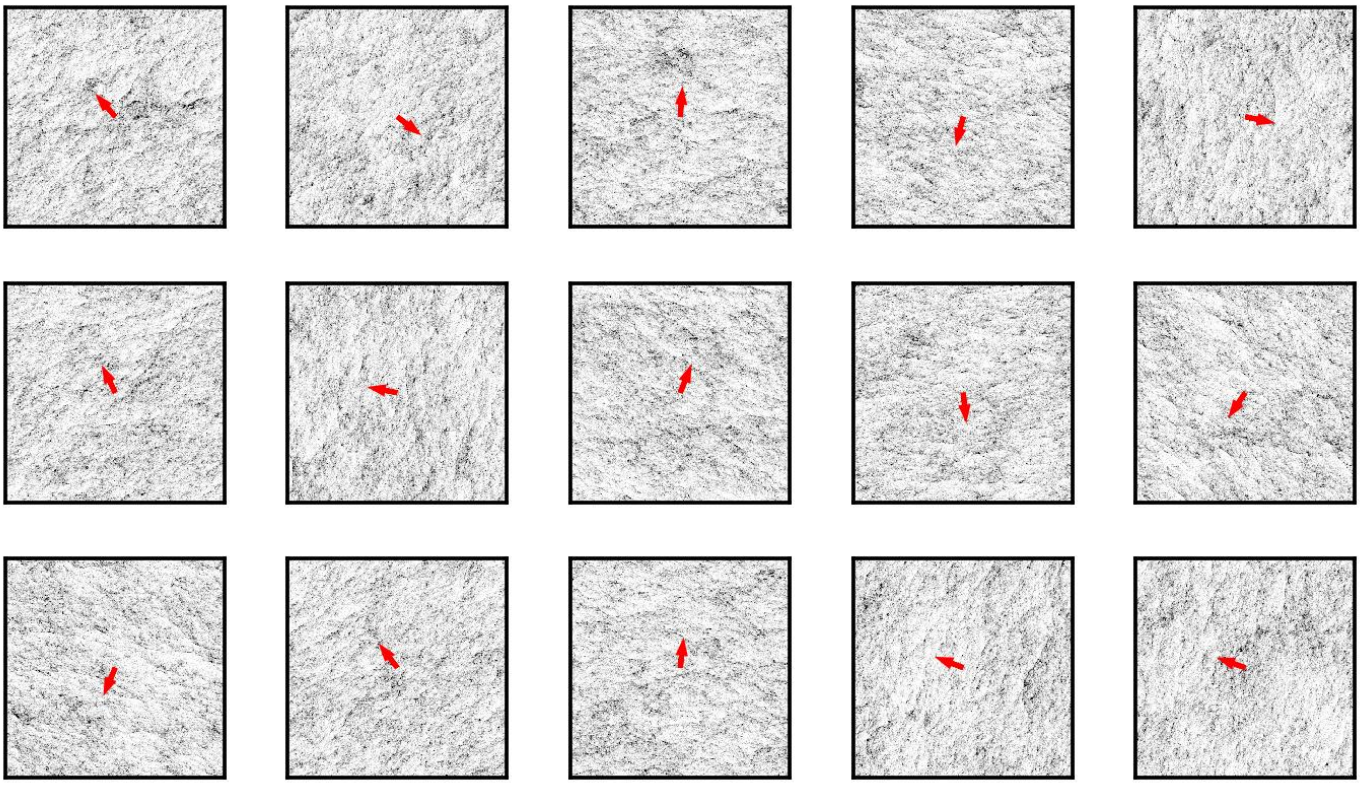

$\eta = 0.22$.

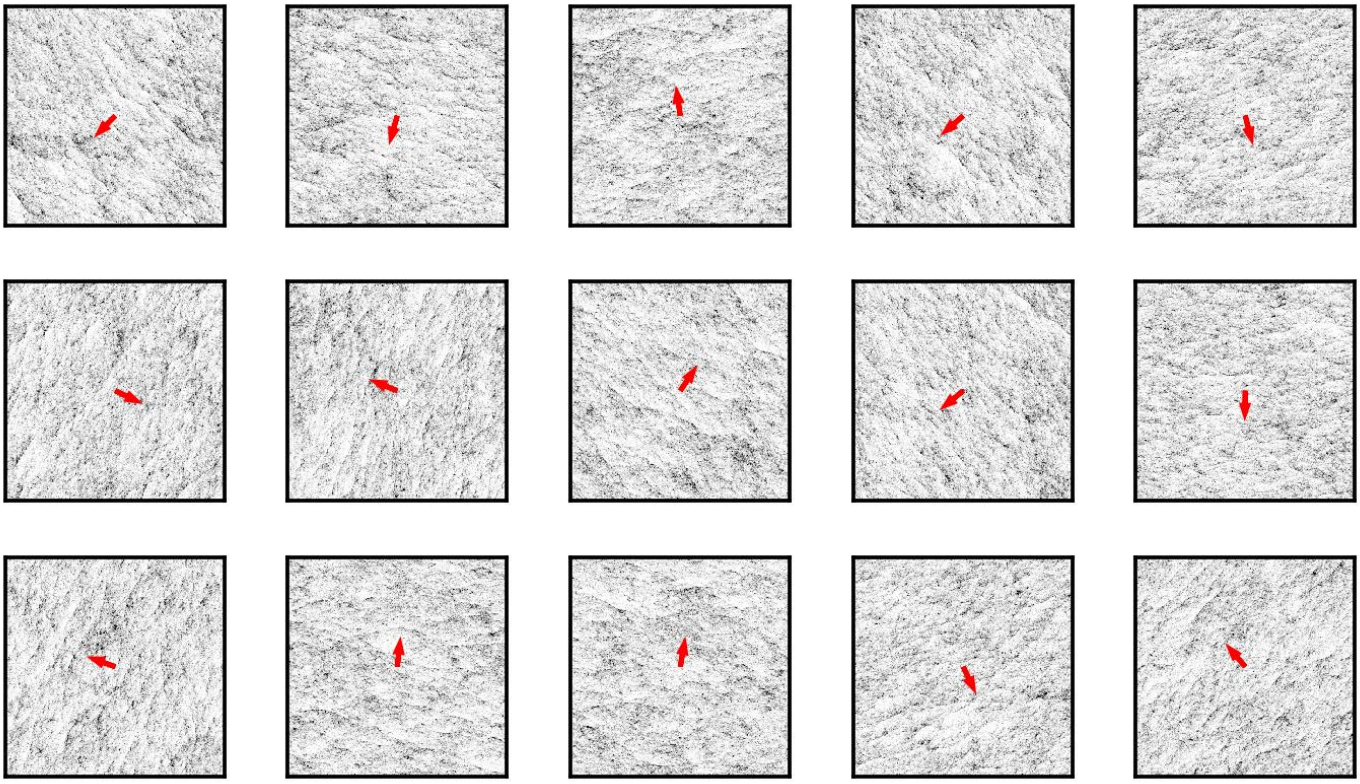

$\eta = 0.23$.

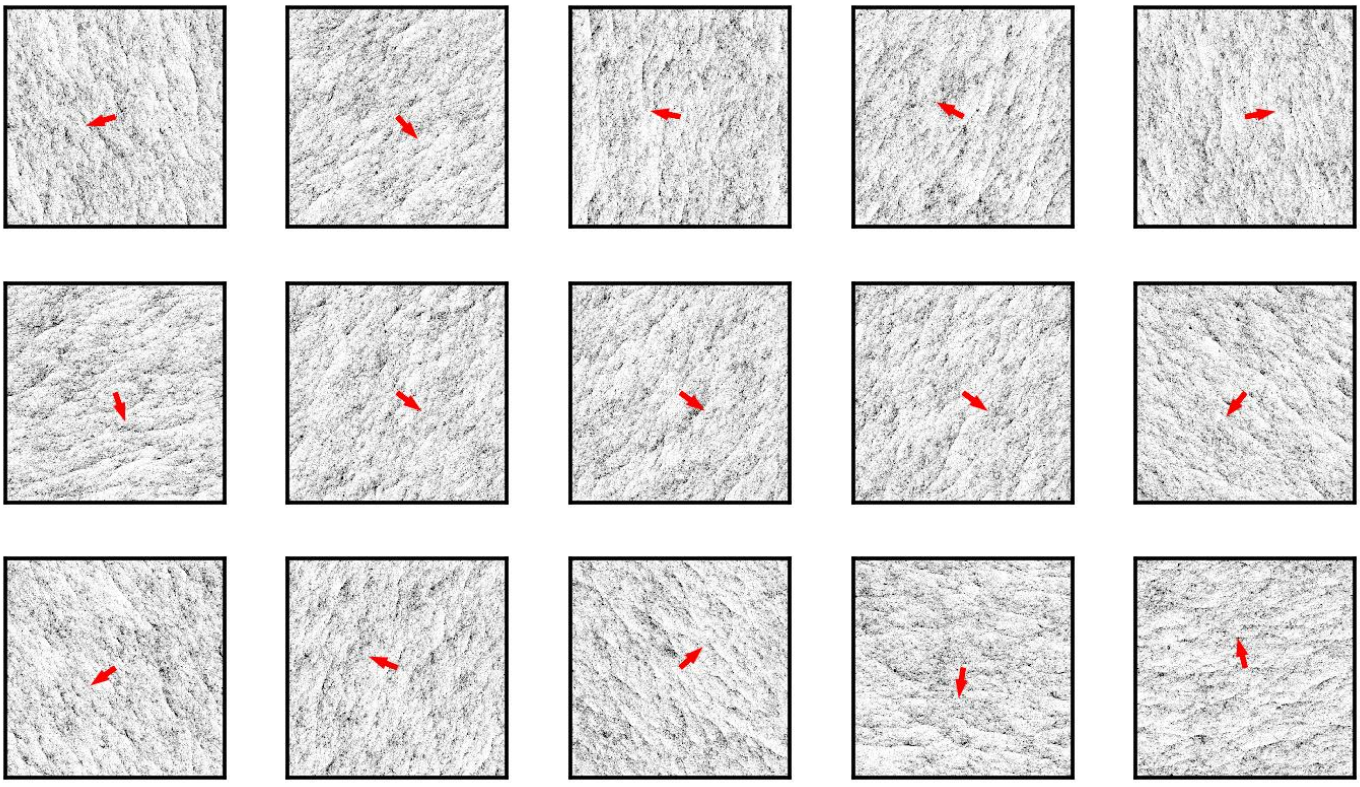

$\eta = 0.24$.

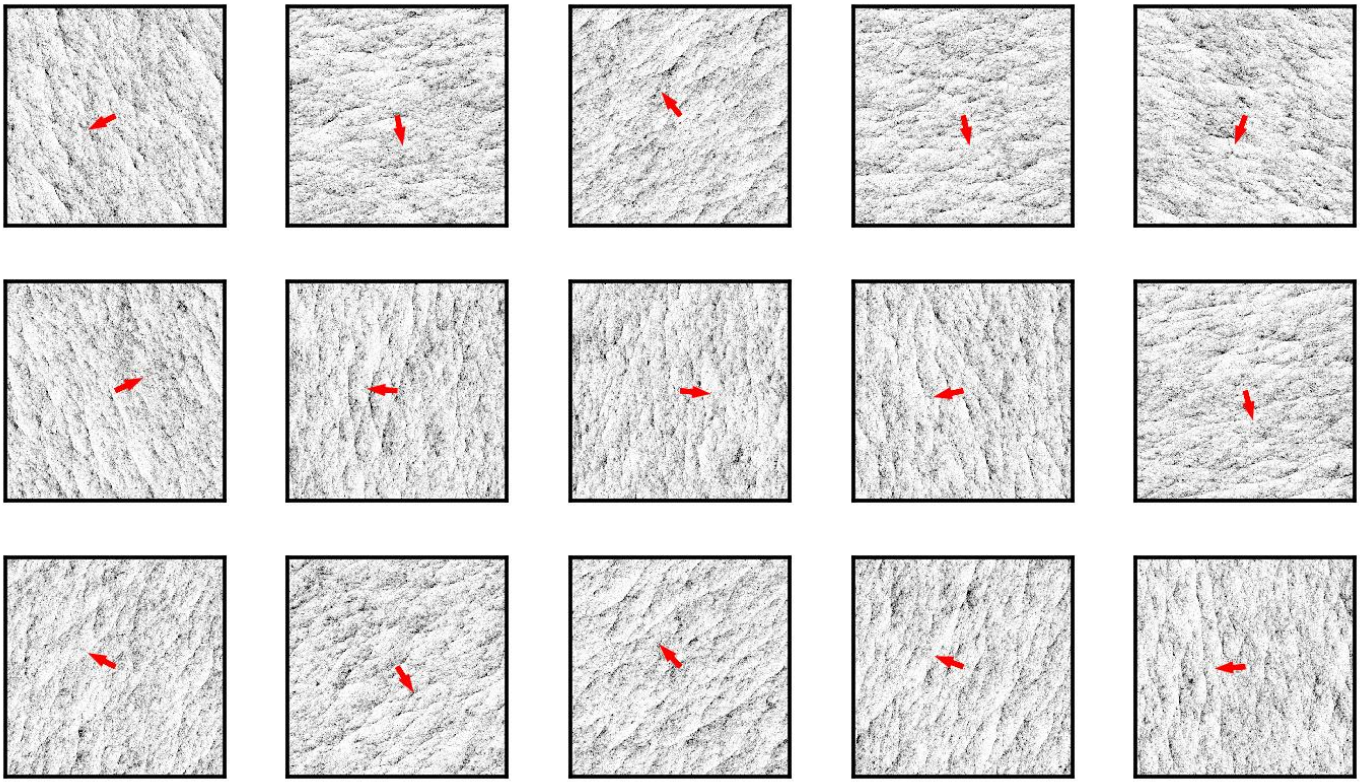

$\eta = 0.25$.

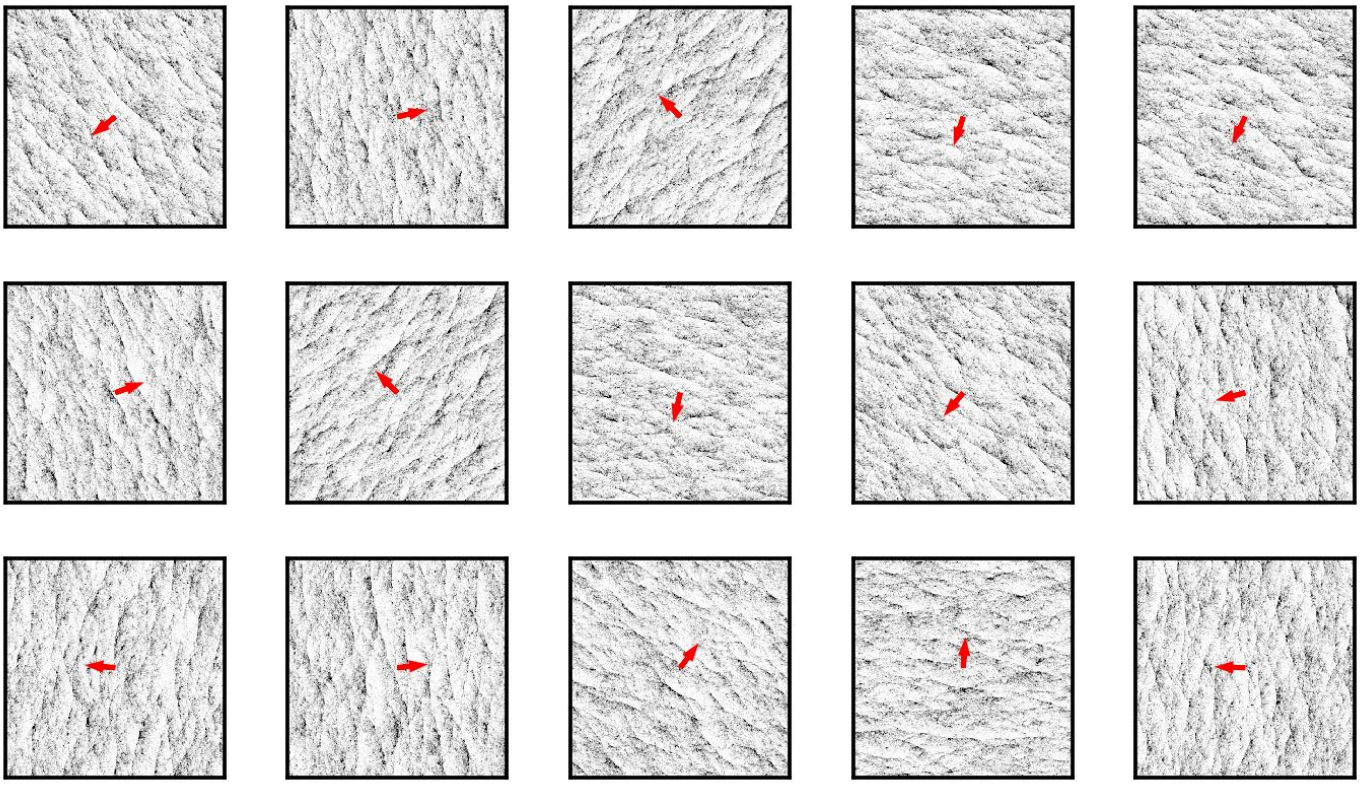

$\eta = 0.26$.

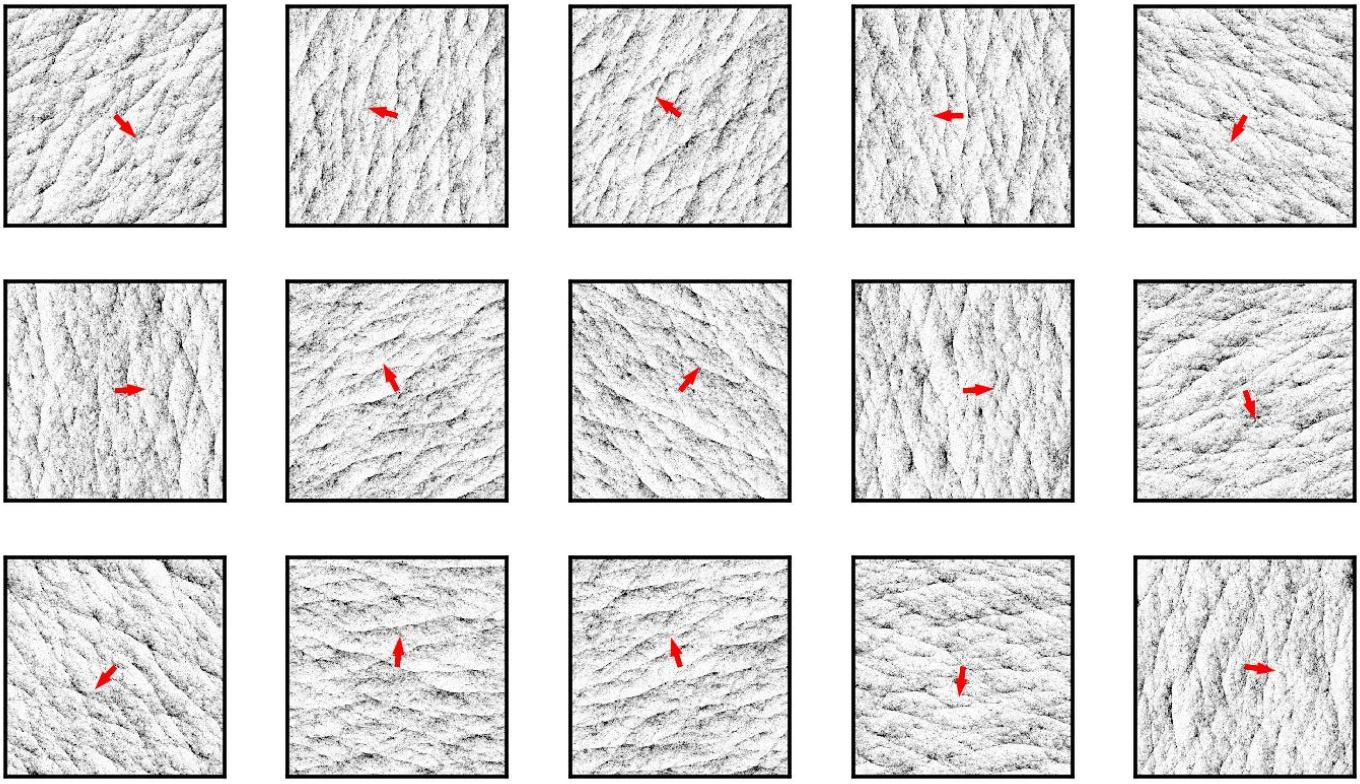

$\eta = 0.27$.

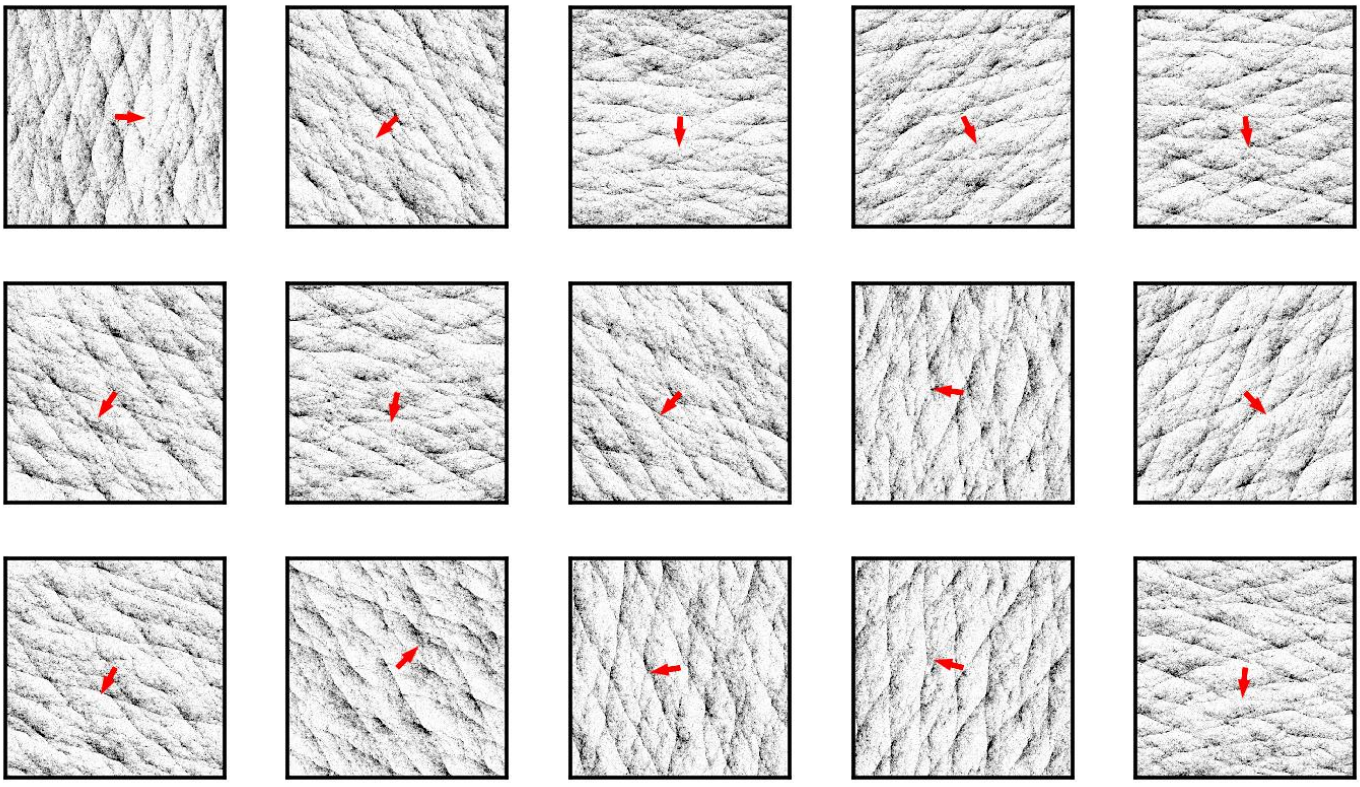

$\eta = 0.28$.

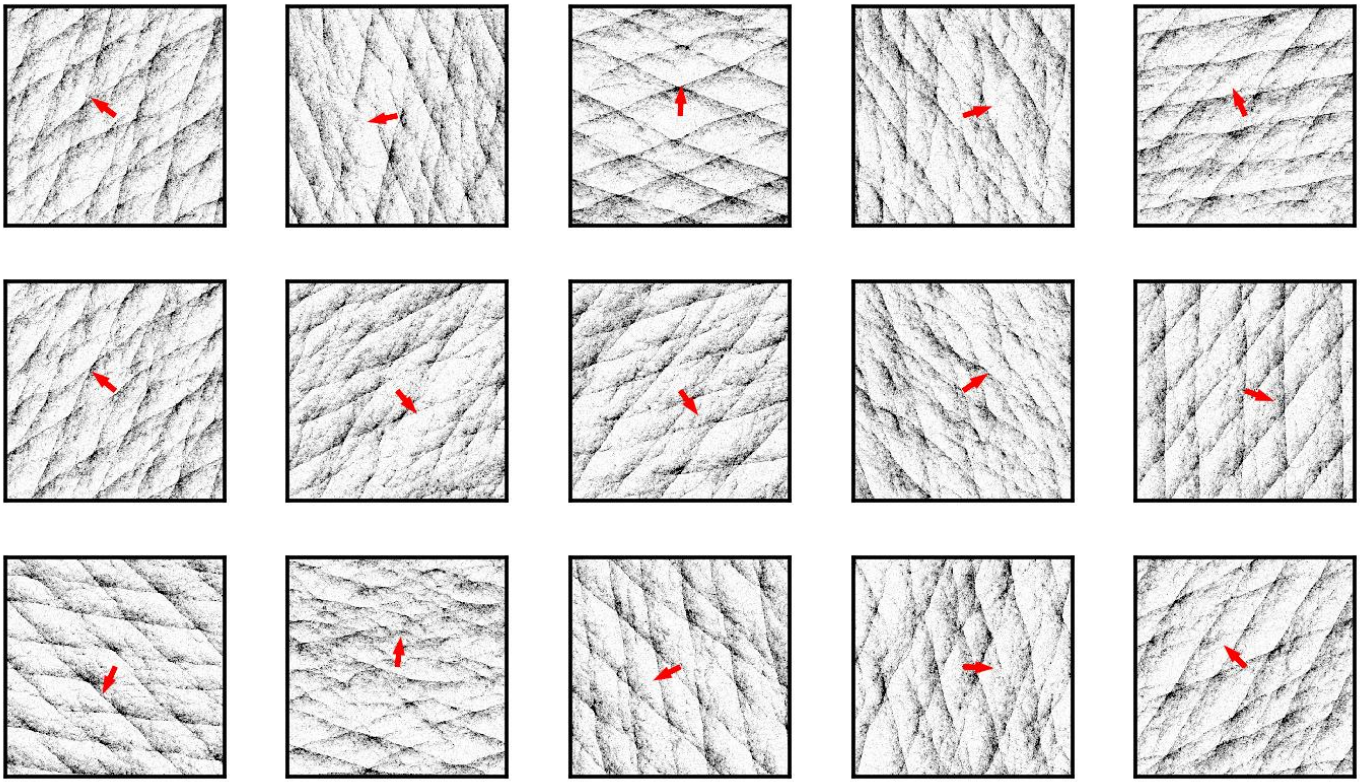

$\eta = 0.29$.

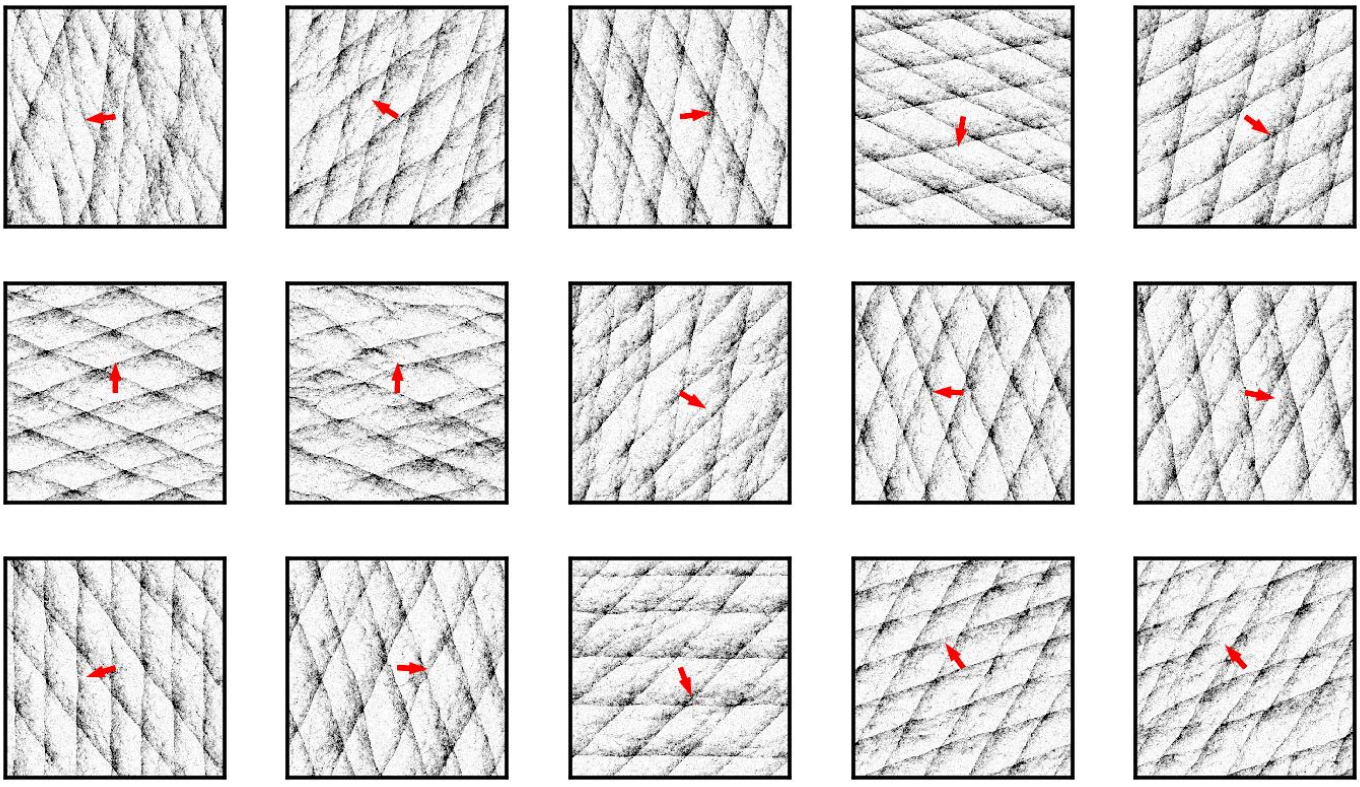

$\eta = 0.30$.

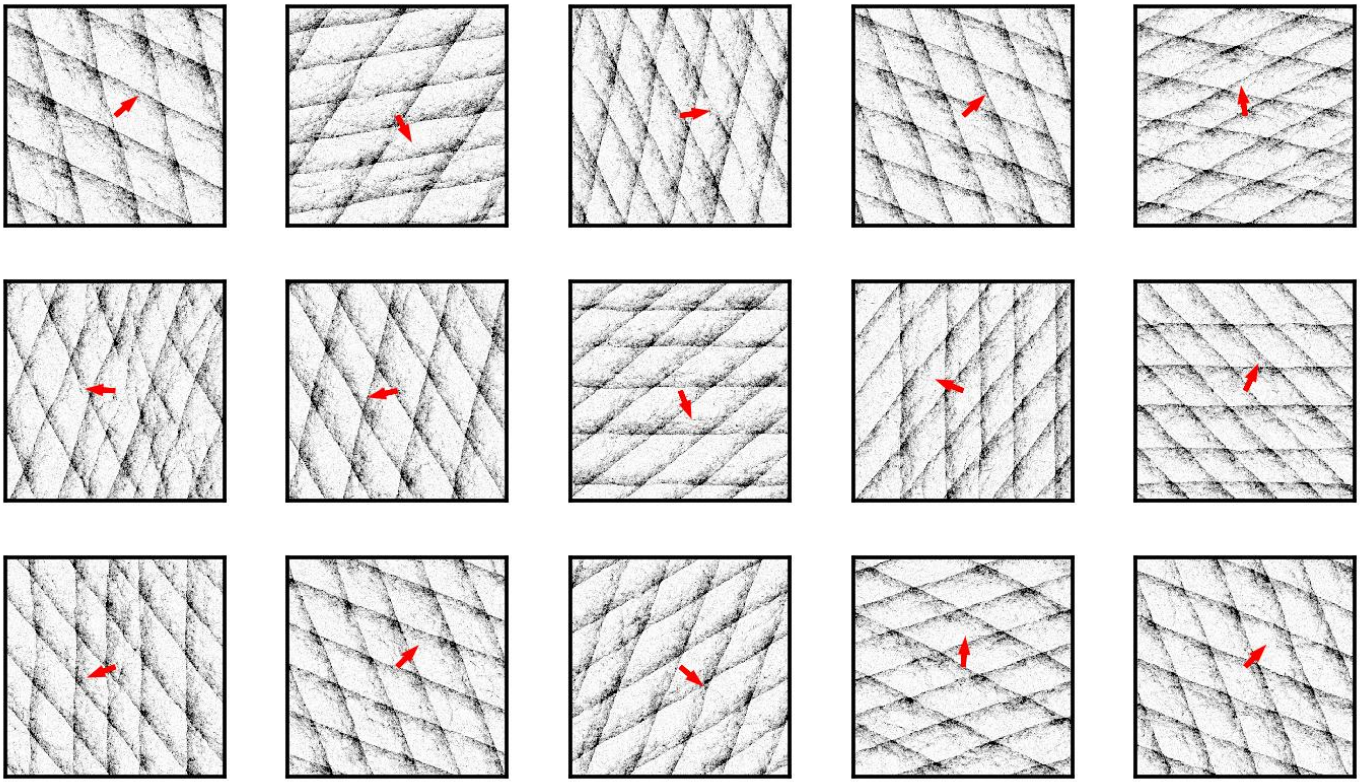

$\eta = 0.31$.

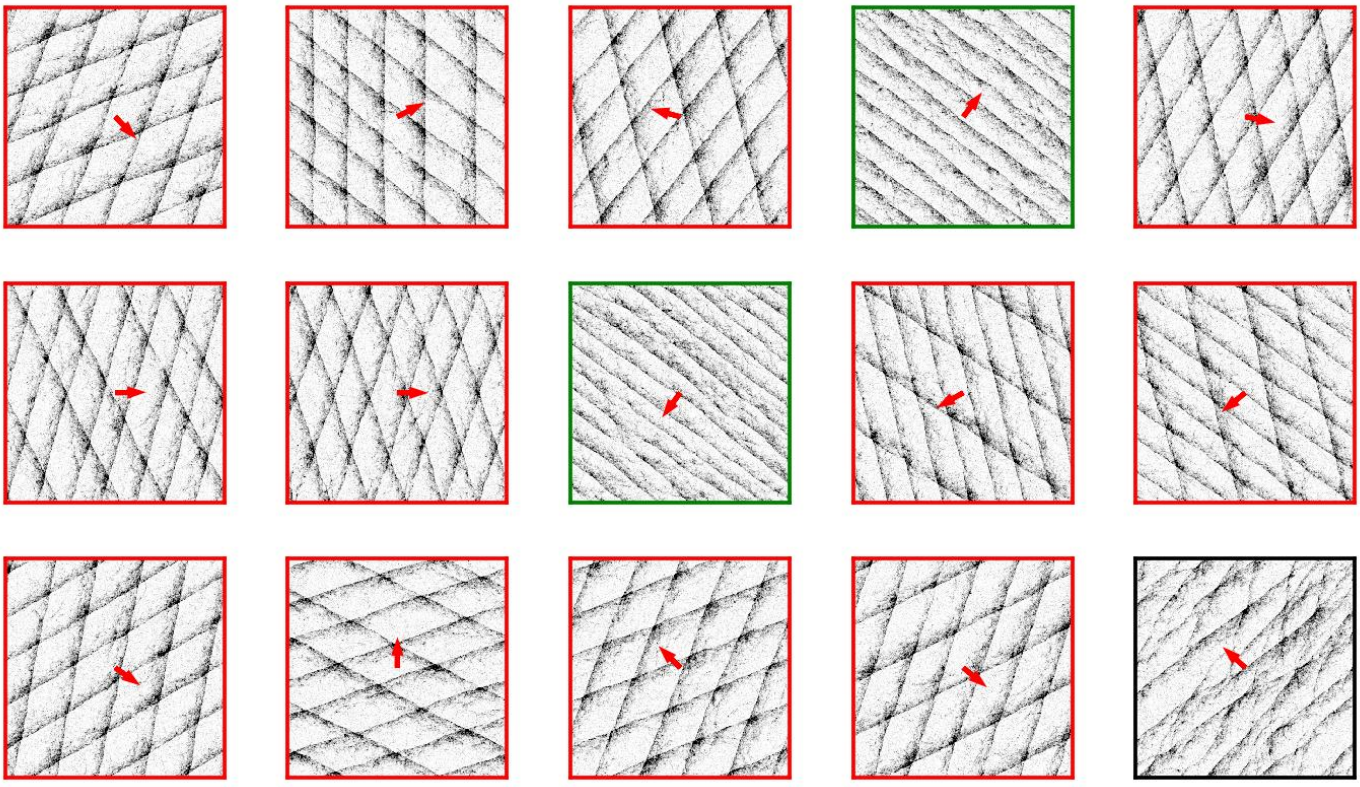

$\eta = 0.32$.

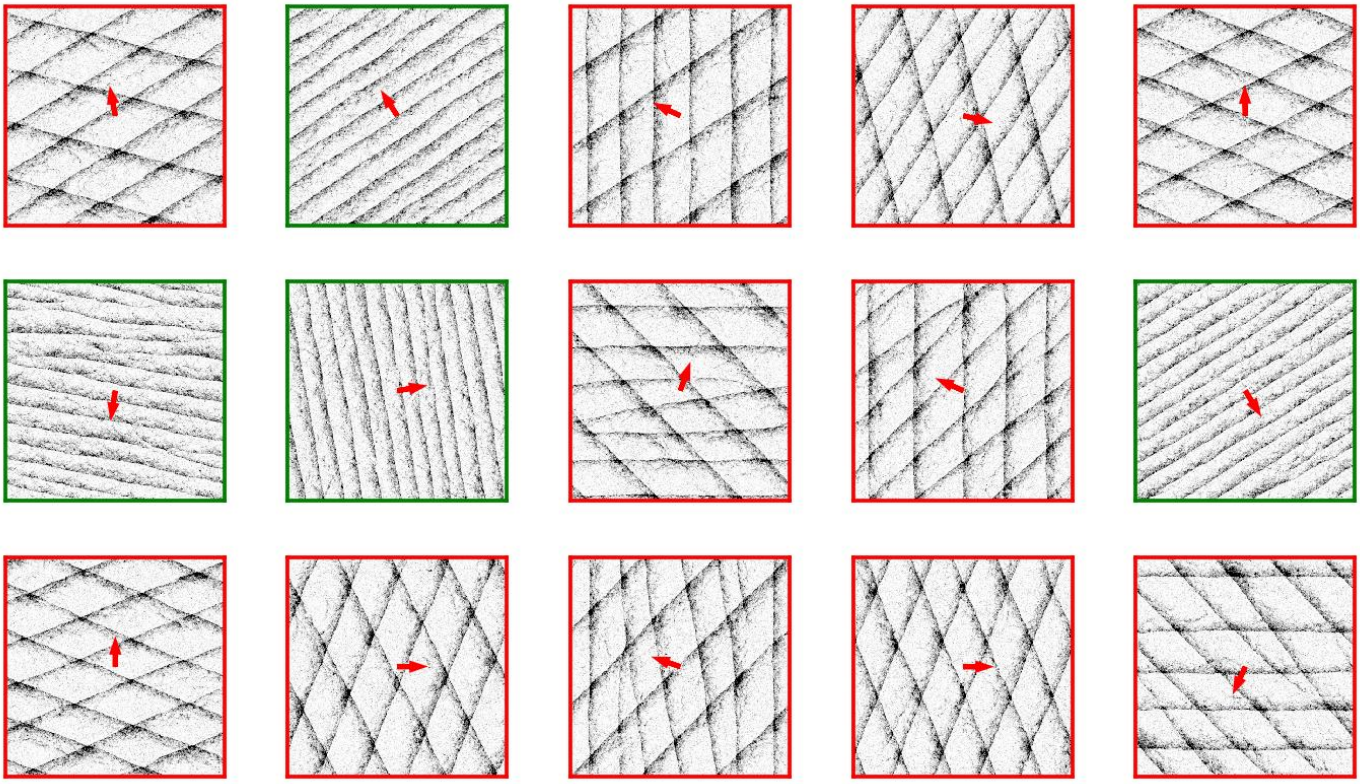

$\eta = 0.33$.

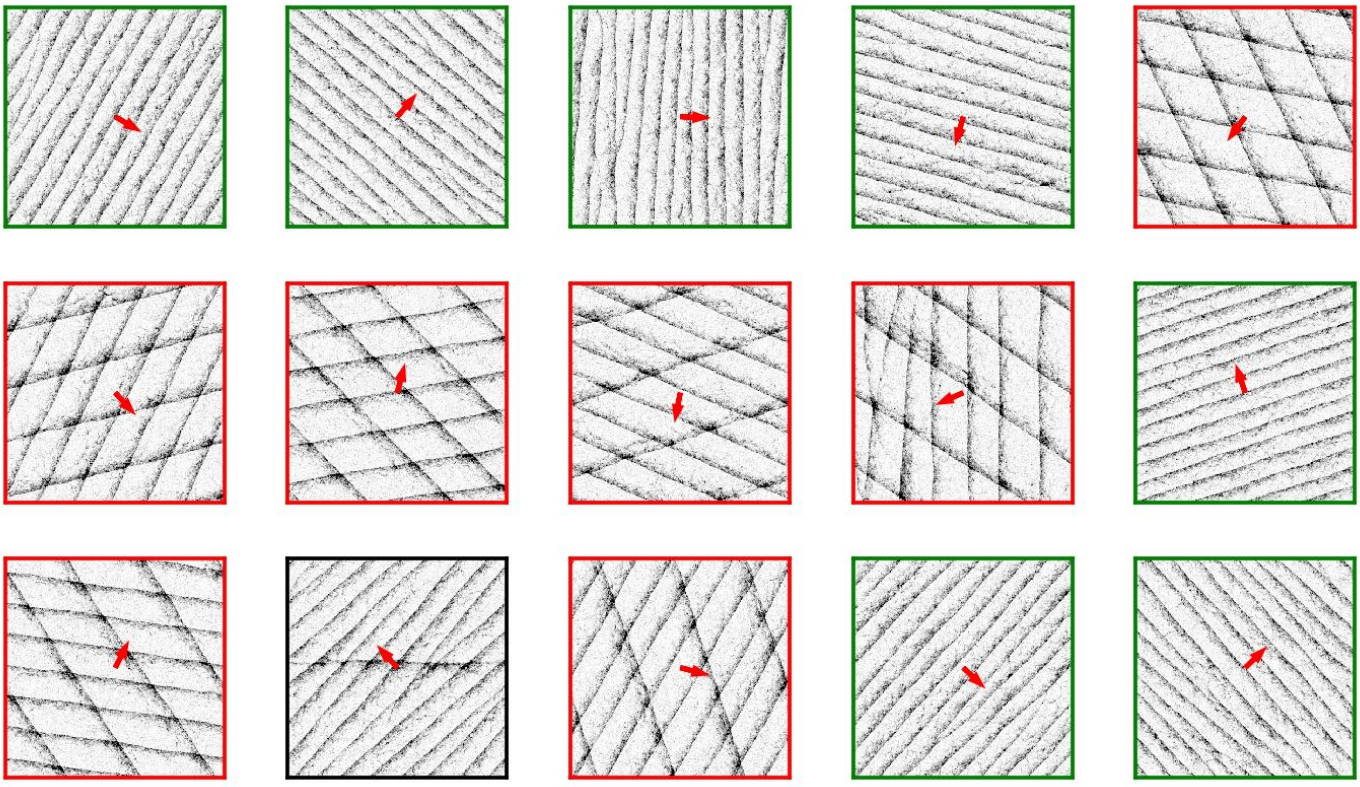

$\eta = 0.34$.

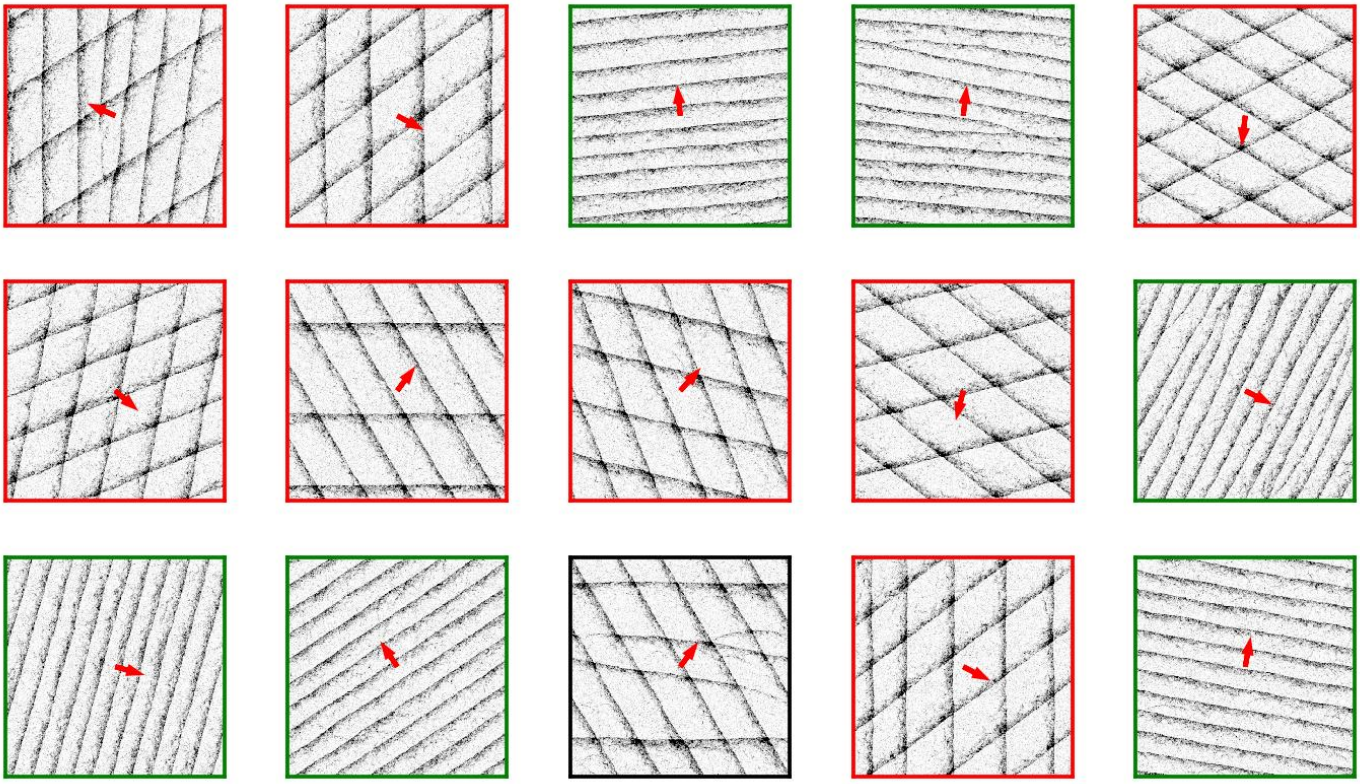

$\eta = 0.35$.

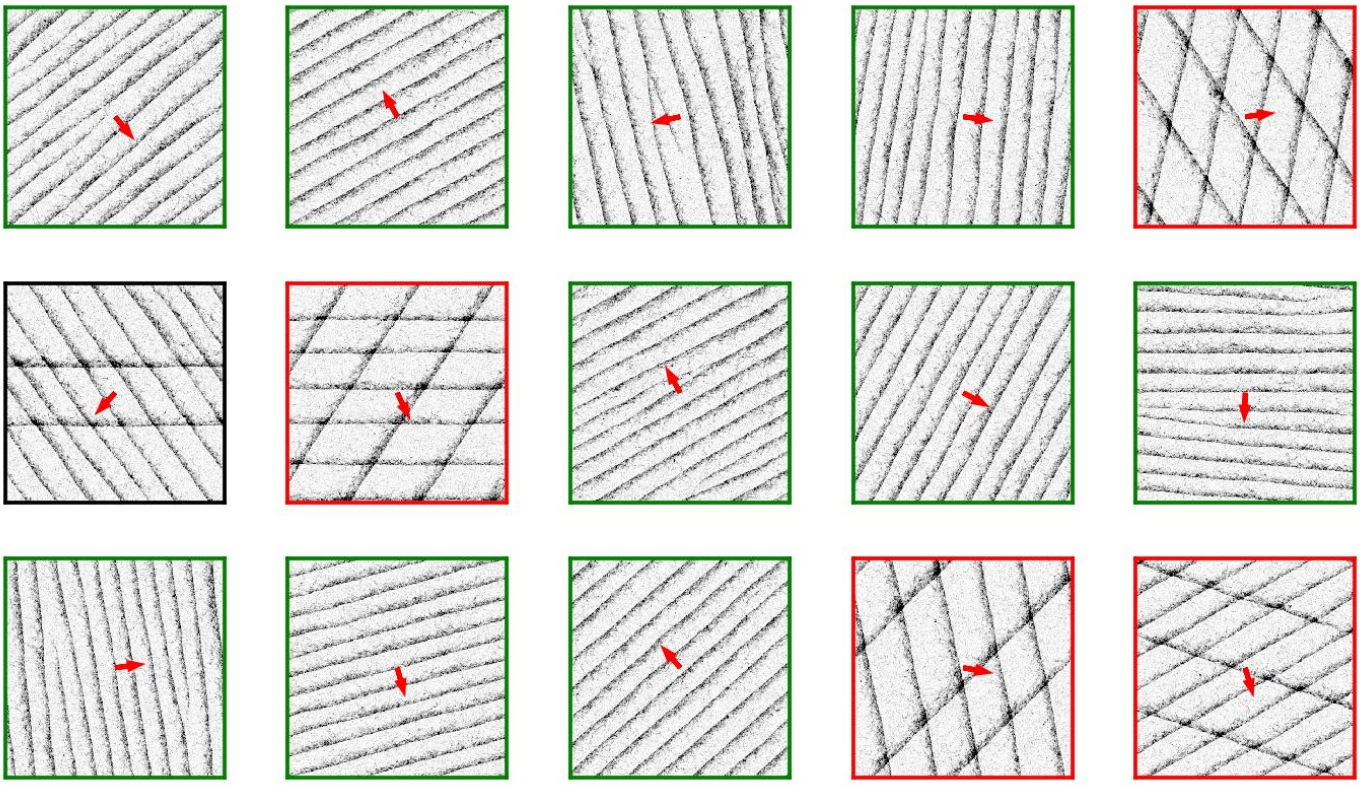

$\eta = 0.36$.

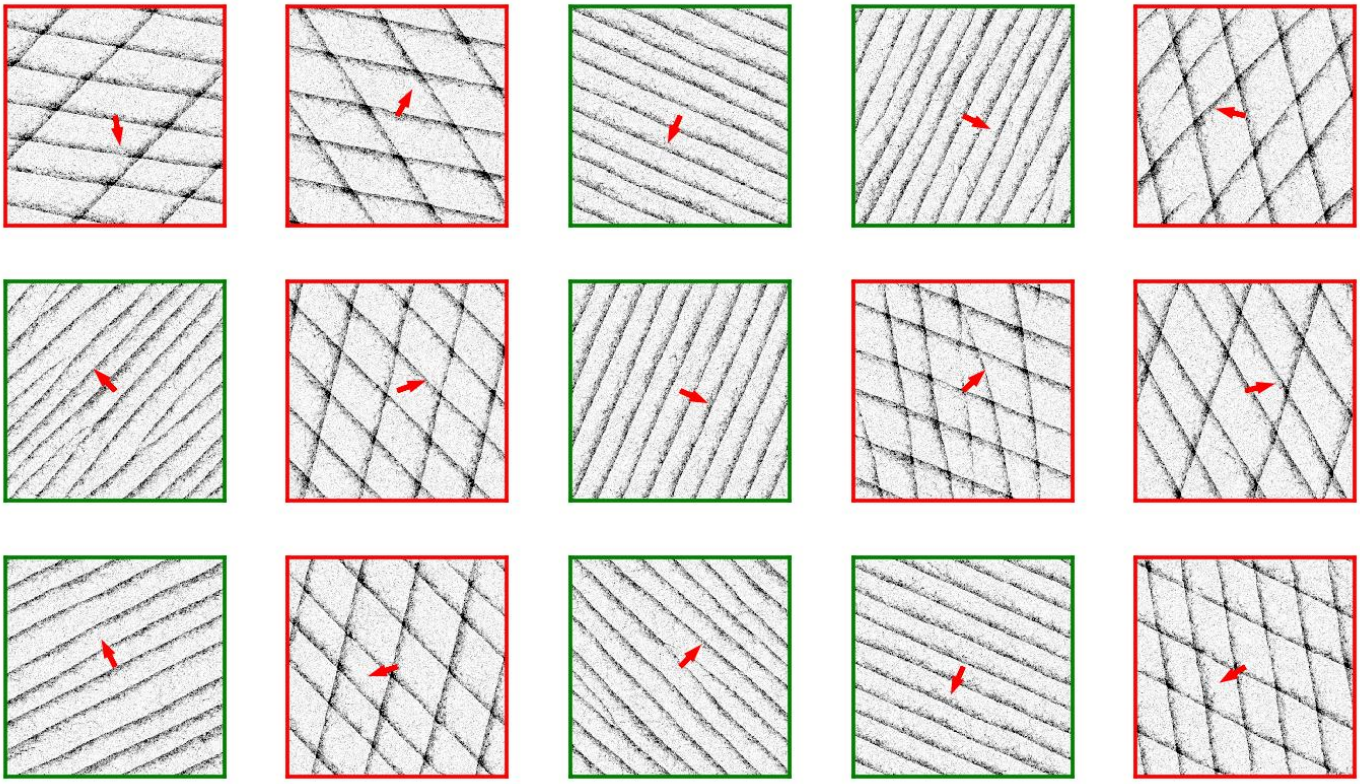

$\eta = 0.37$.

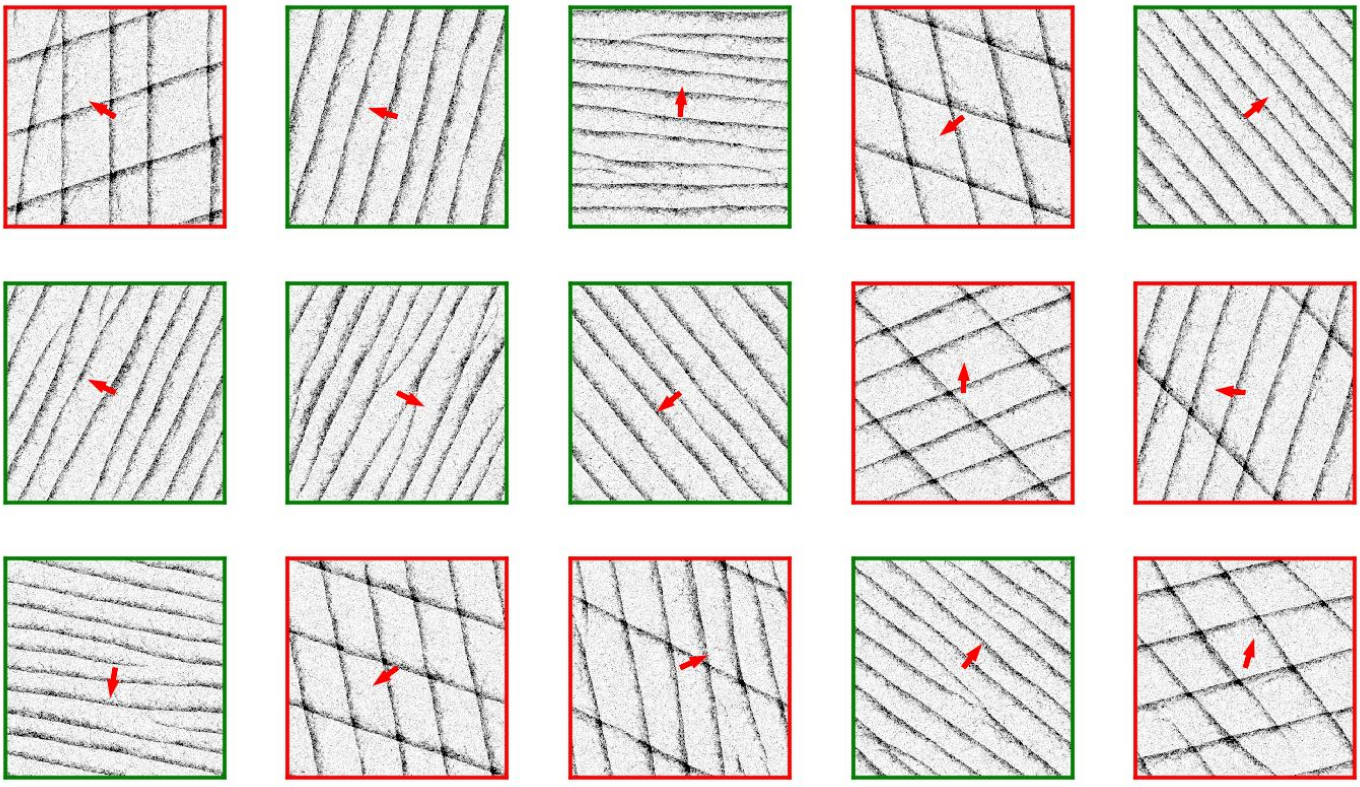

$\eta = 0.38$.

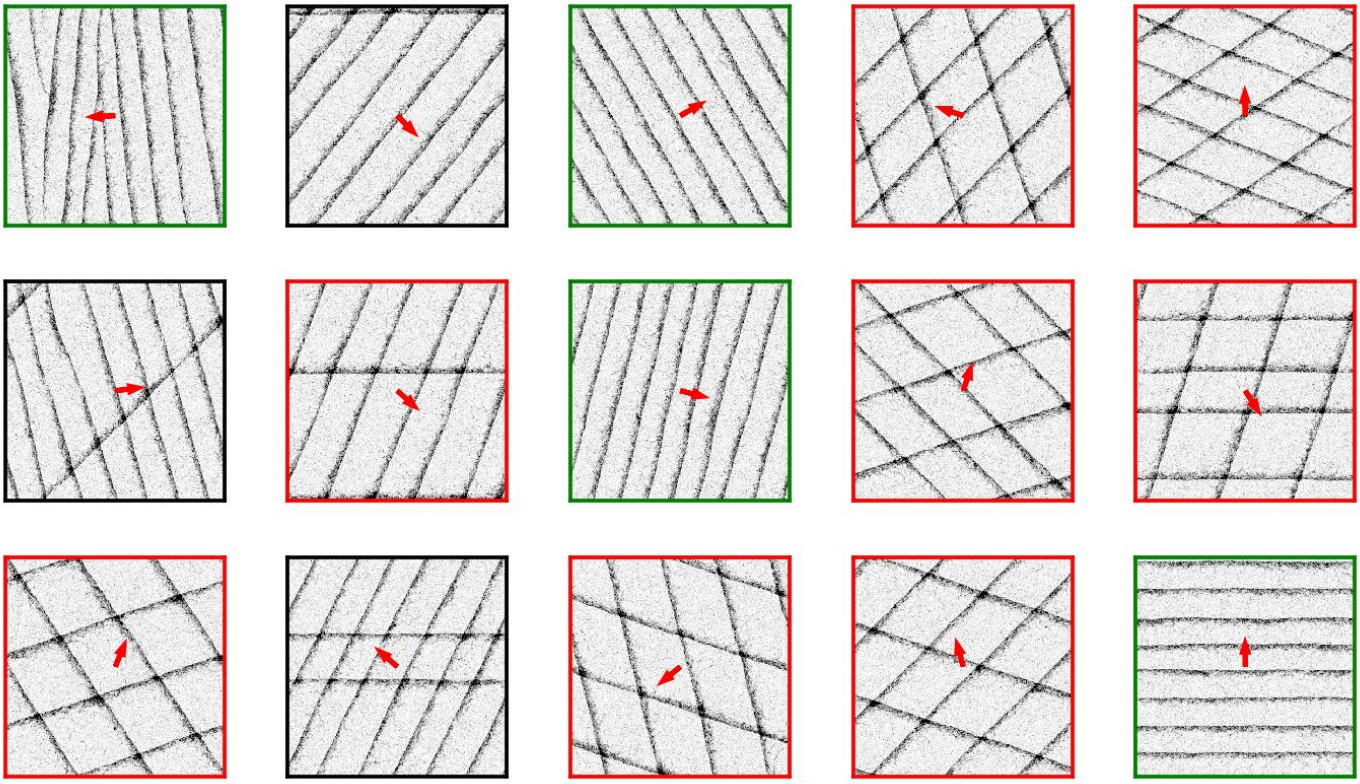

$\eta = 0.39$.

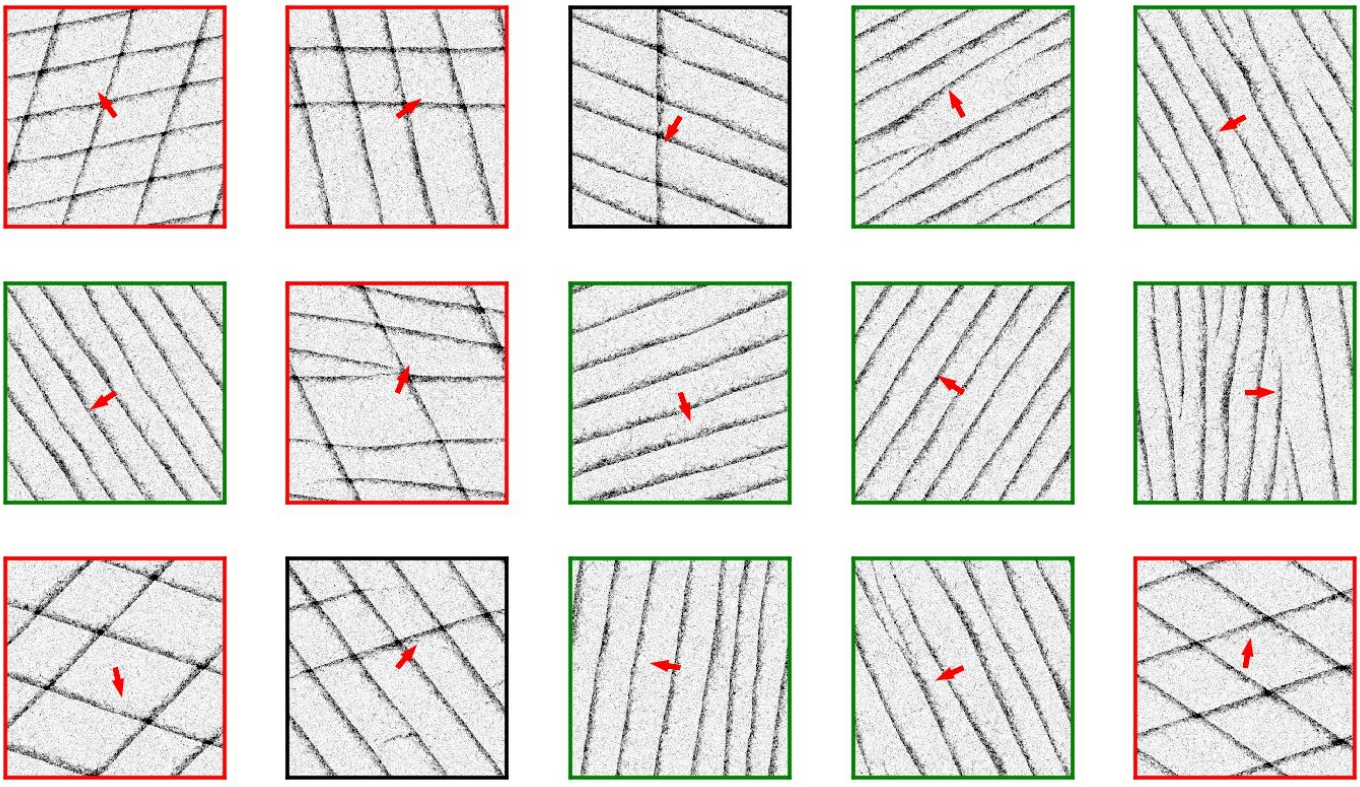

$\eta = 0.40$.

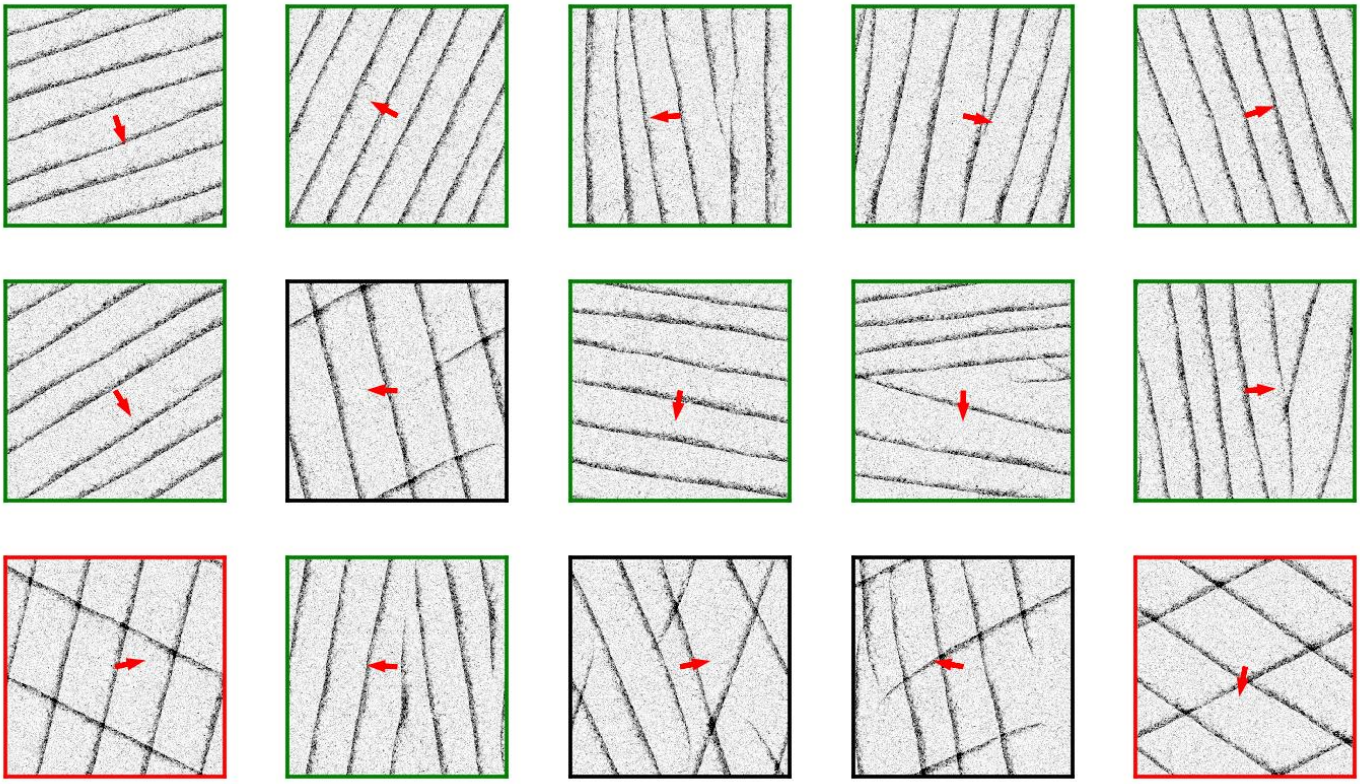

$\eta = 0.41$.

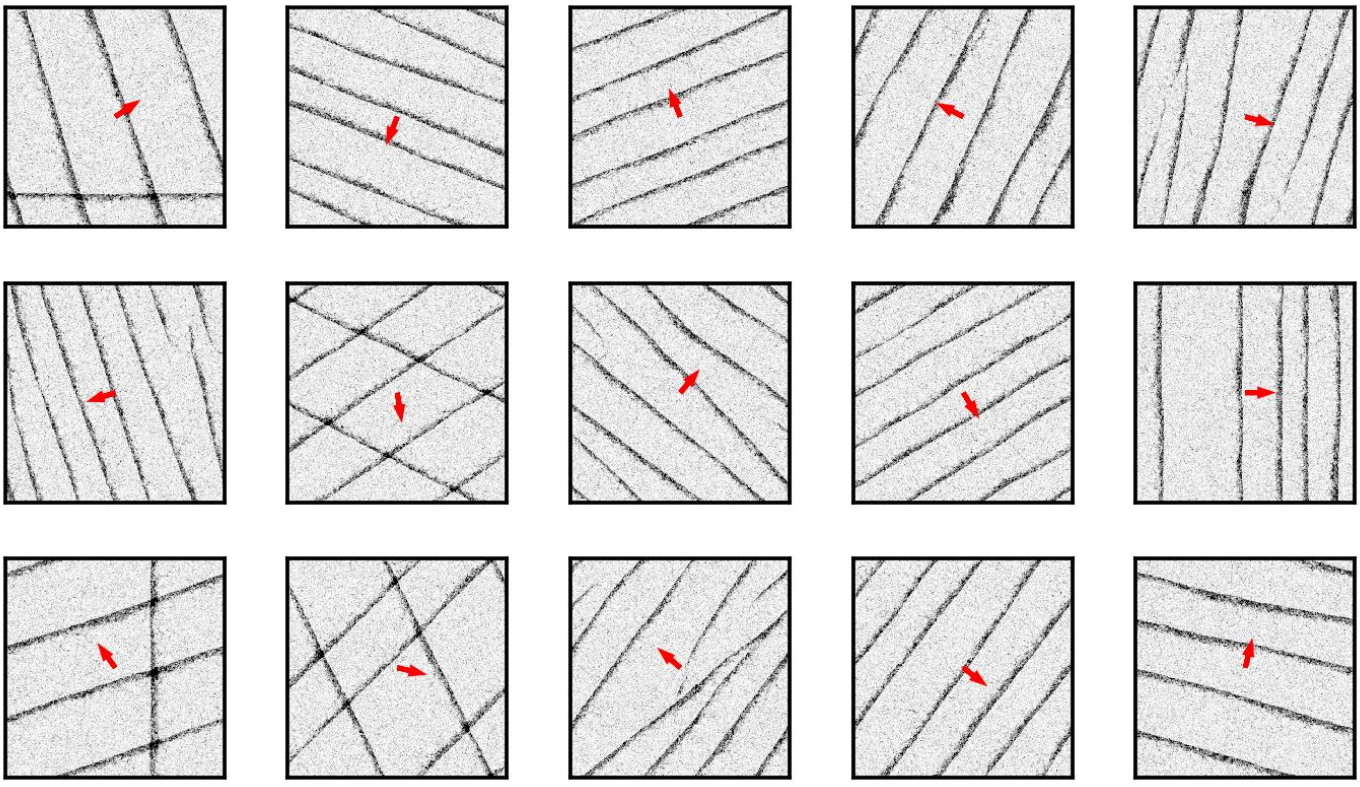

$\eta = 0.42$.

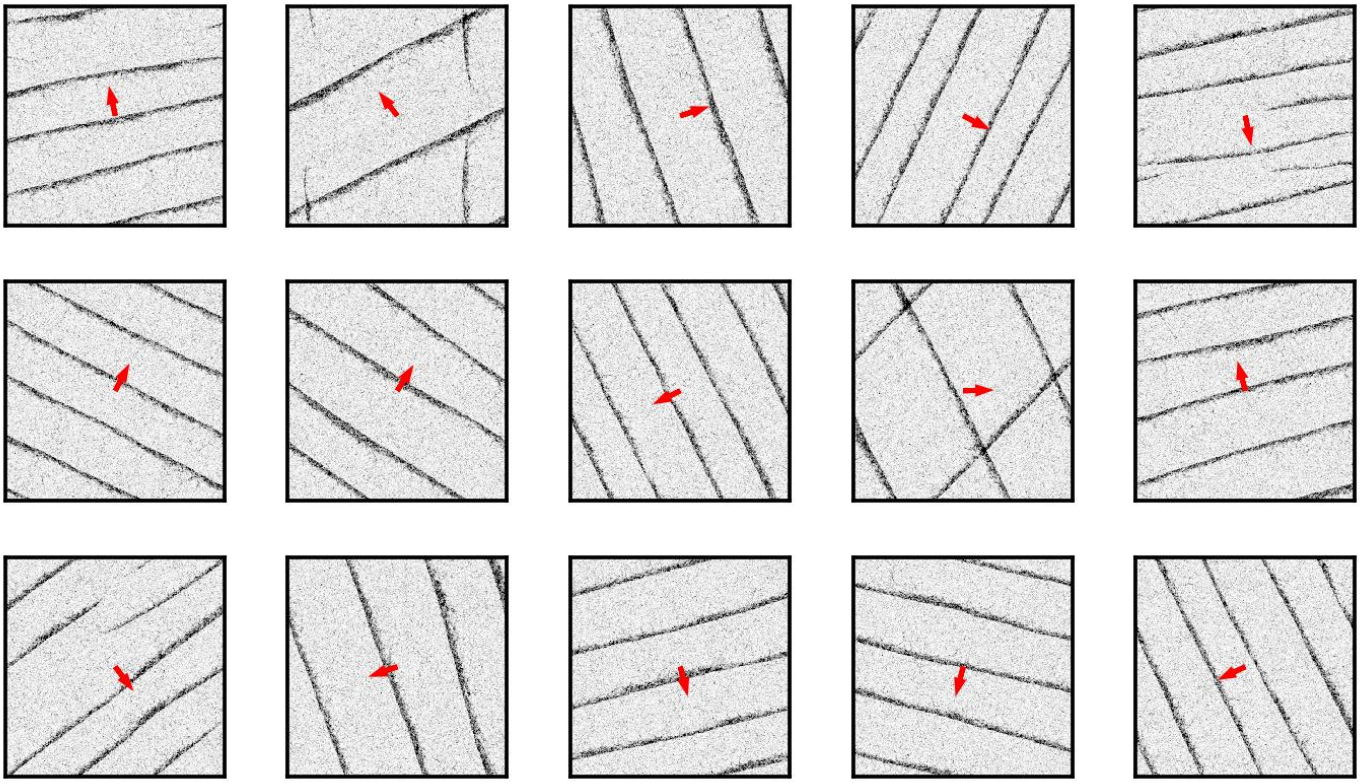

$\eta = 0.43$.

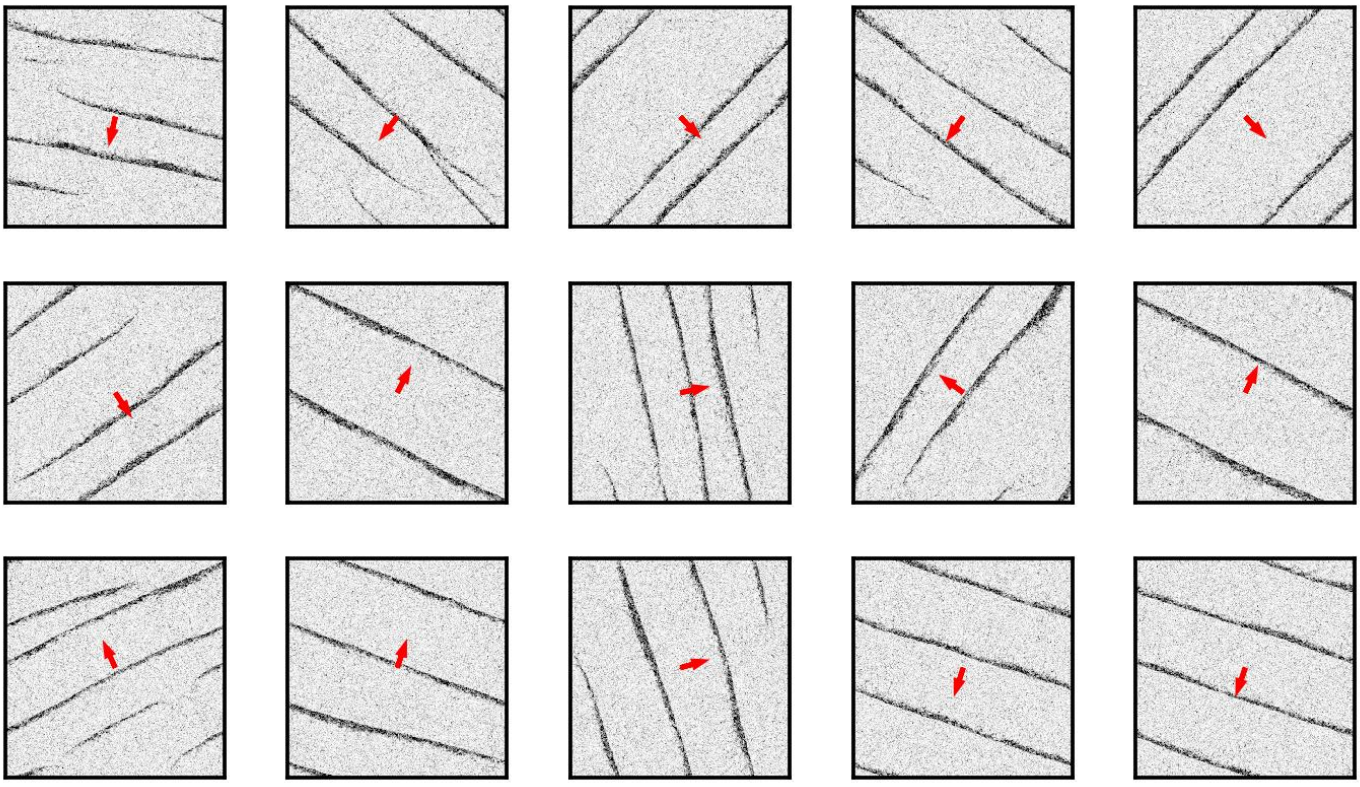

$\eta = 0.44$.

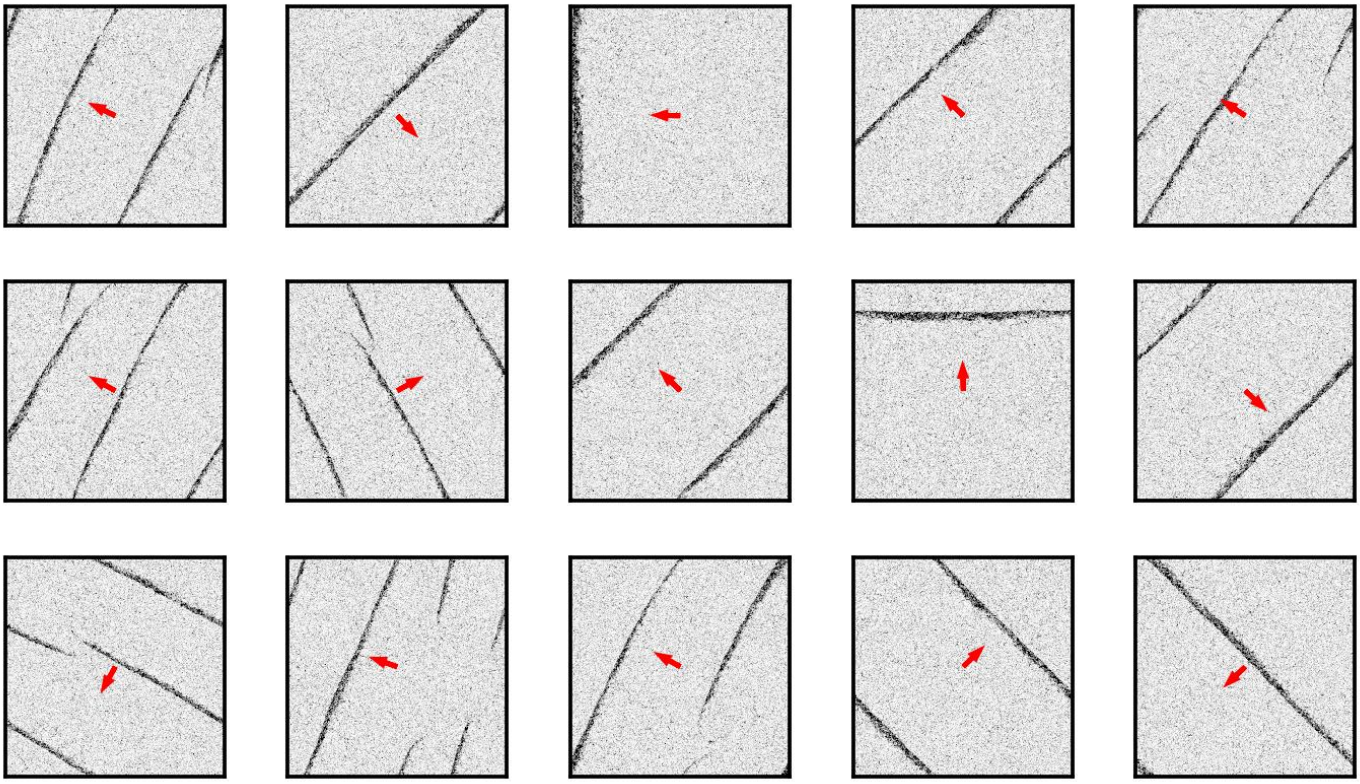

$\eta = 0.45$.

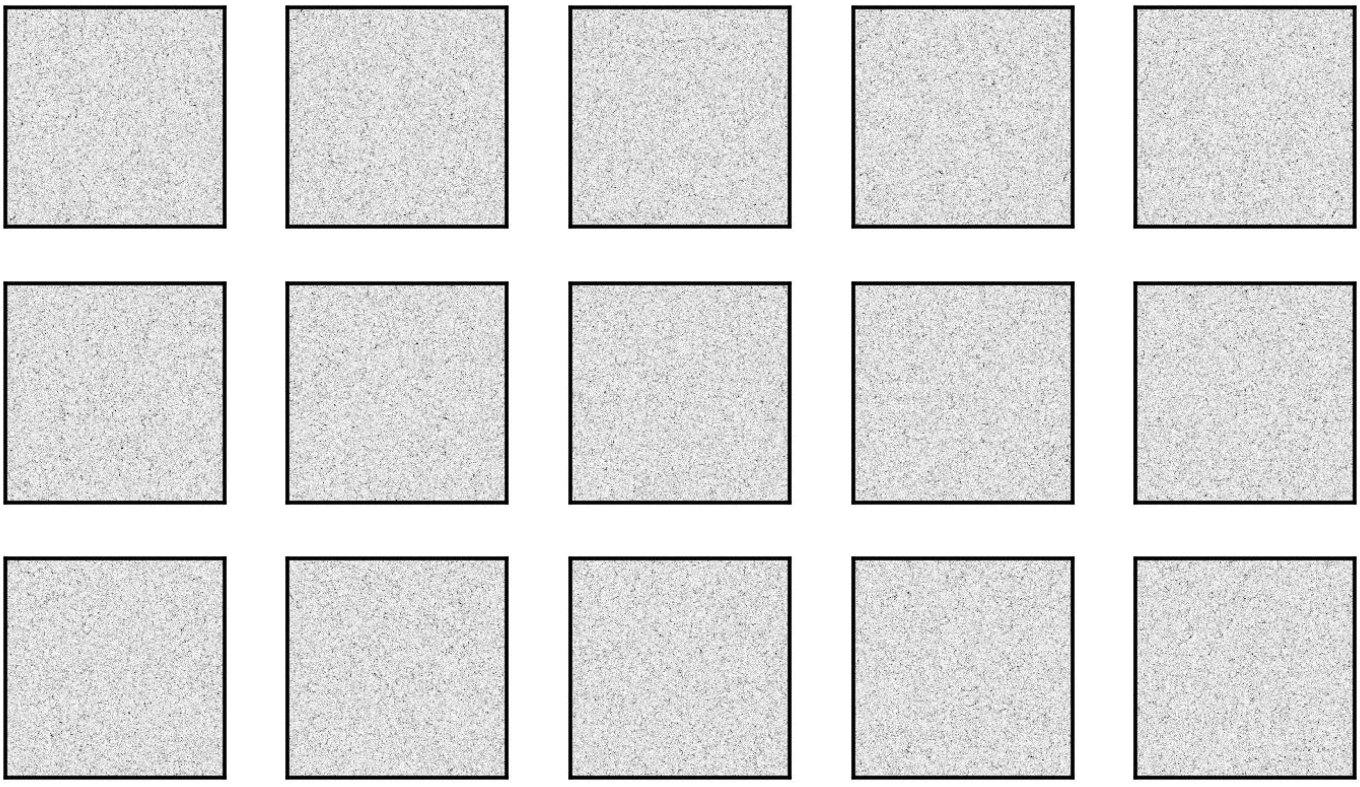

7 Further Parameter Sets

Our main analysis is based on numerical simulations of the standard Vicsek model for different noise strength for one particular parameter set: $N = 10^6$, $L = 1253.3$, $R = 1$, $v = 1$. To make sure that the discovered cross sea phase is in general present within the Vicsek model we investigate also other parameter sets: a larger system, different aspect ratios of the simulation box, a different particle density.

Except for very small aspect ratios (1 : 16) we find completely equivalent results in all those cases. Only for channel-like simulation boxes, the cross sea phase seems to be suppressed in some cases, depending on orientation of the pattern. This is reasonable since the simulation box is simply too small in one direction to fit the cross sea pattern.

7.1 A Larger System: $N = 2 \times 10^6$

In this subsection we show simulation results of the following parameter set: $N = 2\times10^6$, $L = \sqrt{2}\times1253.3 \approx 1772.5$, $R = v = 1$. That are the same parameters as in the Letter but for a larger system size (at the same density). Because we are mainly interested in the cross sea phase, we investigate only noise strengths from $\eta = 0.25$ to $\eta = 0.38$ in steps of 0.01. Thus, we do not cover the transition between band phase and disorder. The results are very similar to the smaller system reported in the Letter. In Fig. S12 (a) we display the C_2 order parameter averaged over 15 realizations and 10^4 time steps for each realization after a thermalization time of 2×10^5 time steps. In Fig. S12 (b) we show the corresponding Binder cumulant. The vertical lines are at the transition noise strengths η_{c1} and η_{c2} of the Letter. We see that the transition between phases (ii) and (iii) is (within our resolution) at exactly the same point as for the smaller system. To sample the other transition between phases (i) and (ii) we would need a higher resolution in noise strength and much more realizations, which is beyond our computational resources. One might forebode that this transition is slightly shifted towards smaller noise strengths for the larger system.

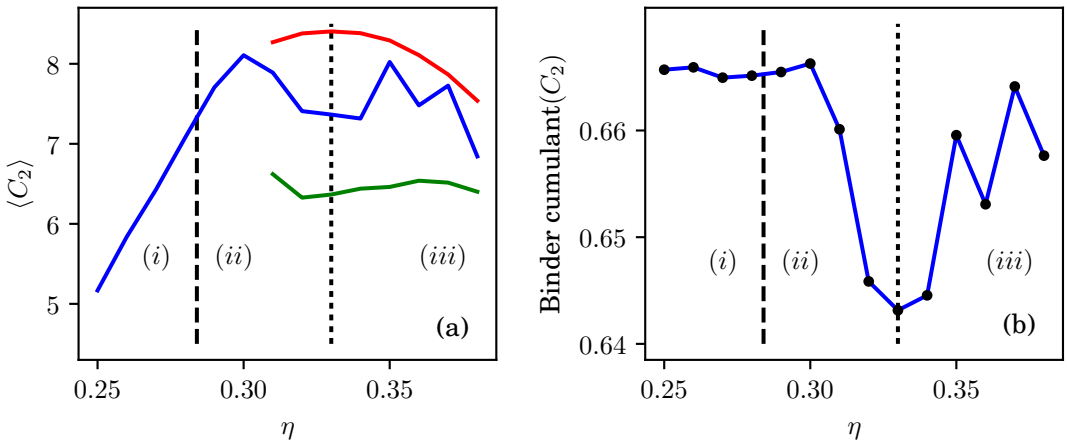

Figure S12: (a) Structural order parameter C_2 obtained from all realizations (blue line) and averaged only over cross sea (red line) or band (green line) realizations. (b) Binder cumulant of C_2. The dashed vertical lines show the transition noise strengths η_{c1} and η_{c2} from the Letter.

Also here, we can clearly observe the different phases from snapshots. Here, we do not want to show all the snapshots but restrict ourselves to the three characteristic cases. In the following we show 15 snapshots from the Toner-Tu phase at $\eta = 0.25$,

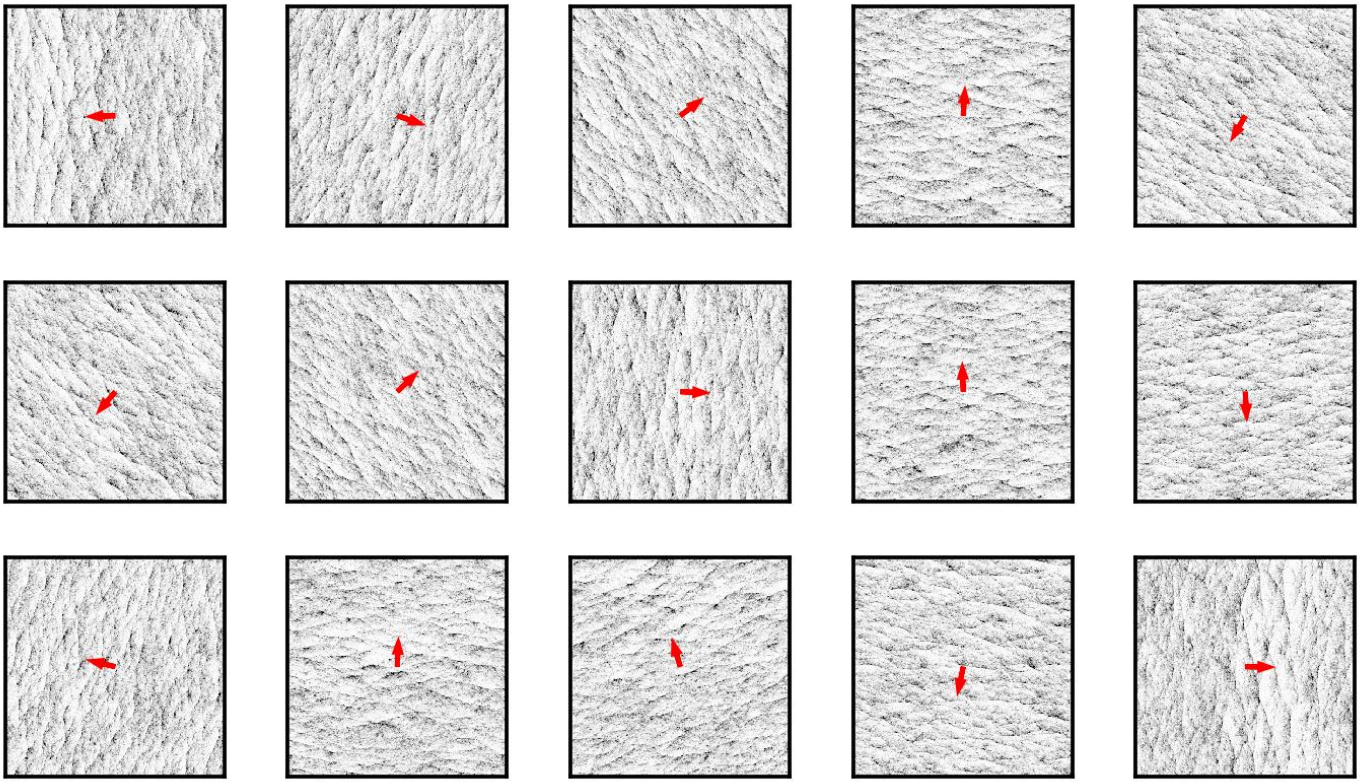

from the cross sea phase at $\eta = 0.30$

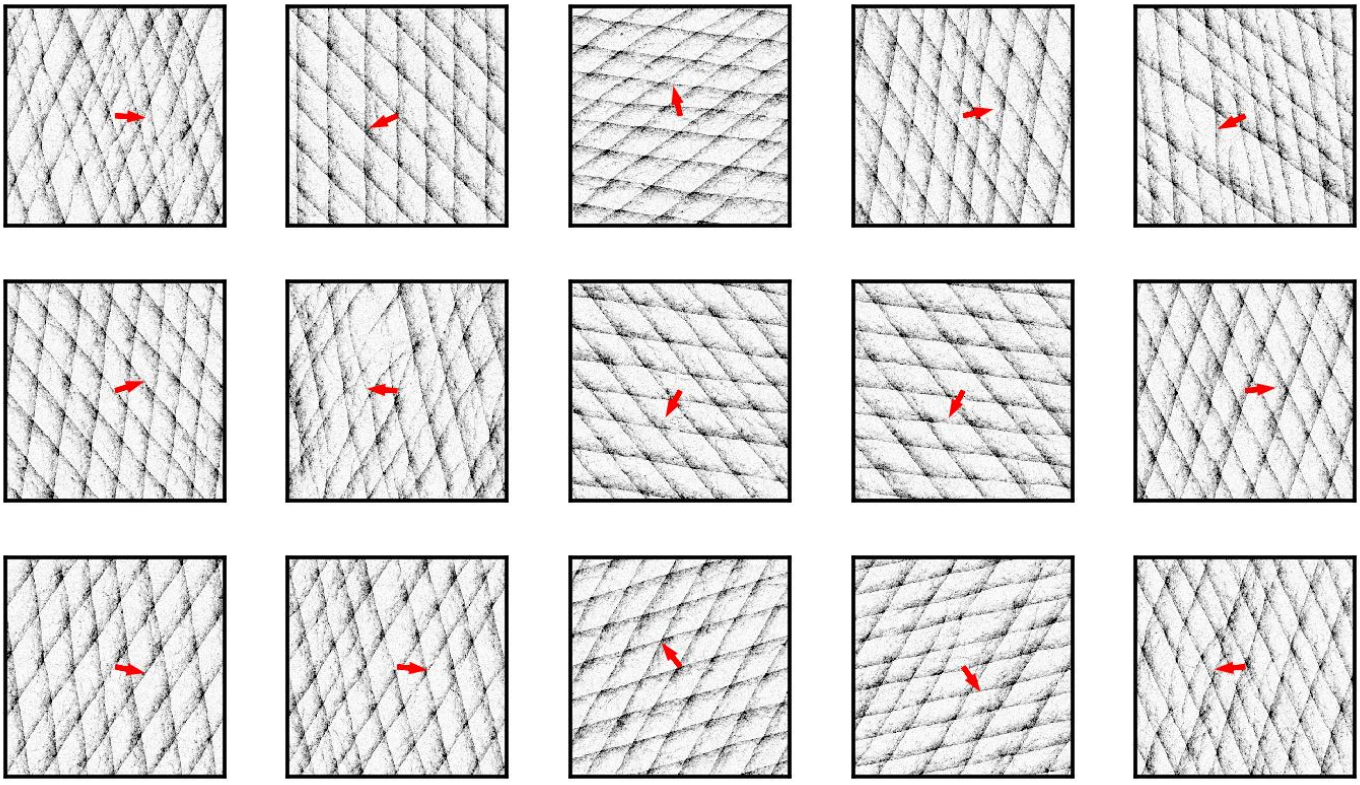

and for $\eta = 0.34$ where some realizations are in cross sea state and some are in band state.

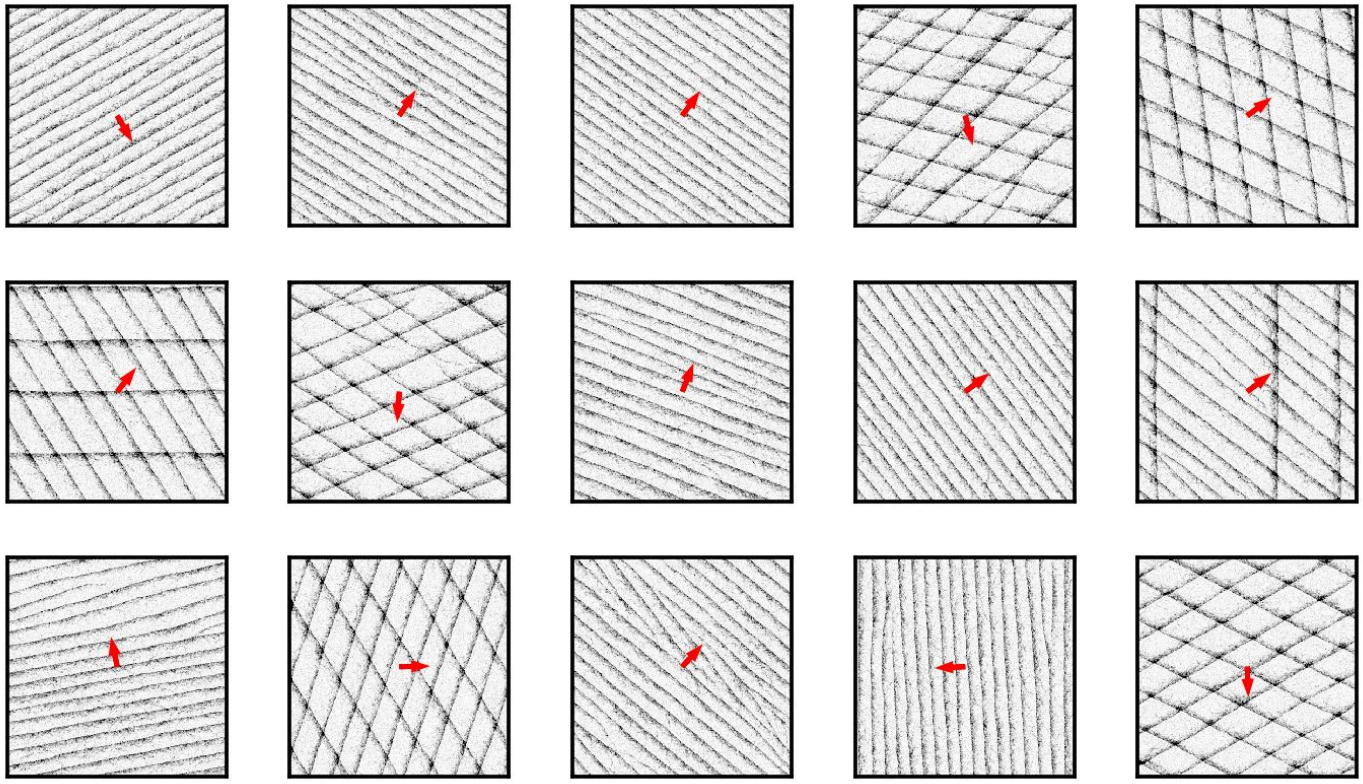

7.2 Aspect Ratio 1 : 4

In this subsection, we present simulation results for the same parameters as in the Letter, but with an aspect ratio of the simulation domain of 1 : 4. That means $L_x = 2506.6$ and $L_y = 626.7$. The measured order parameter is very close to the one sampled on quadratic domains, see Fig. S13 (a). Also the Binder cumulant has minima at the same positions, see Fig. S13 (b).

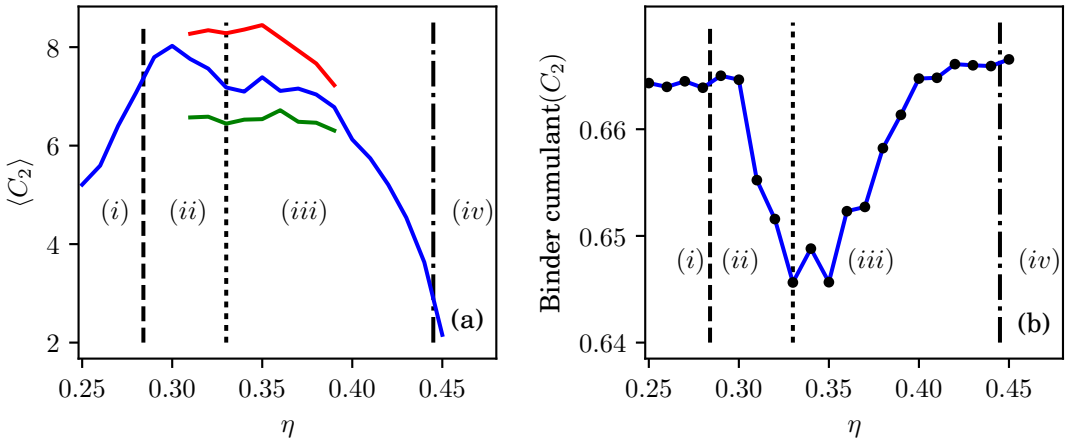

Figure S13: (a) C_2 order parameter and its Binder cumulant (b) for parameters as in the Letter but with an aspect ratio of the simulation box of 1 : 4. Averages have been taken over 15 realizations and 10^4 time steps after thermalizing for 2×10^5 time steps, as in the Letter. The red and green line in (a) show averages over only cross sea and only band realizations, respectively.

Also the snapshots look very similar to those obtained from a quadratic domain. Here, we show examples of only three characteristic cases: the Toner-Tu phase ($\eta = 0.25$), the cross sea phase ($\eta = 0.30$) and at $\eta = 0.35$ with some realizations in a cross sea state and some in a band state. In summary, we find no significant difference between the quadratic domain and a simulation box with an aspect ratio of 1 : 4.

$\eta = 0.25$.

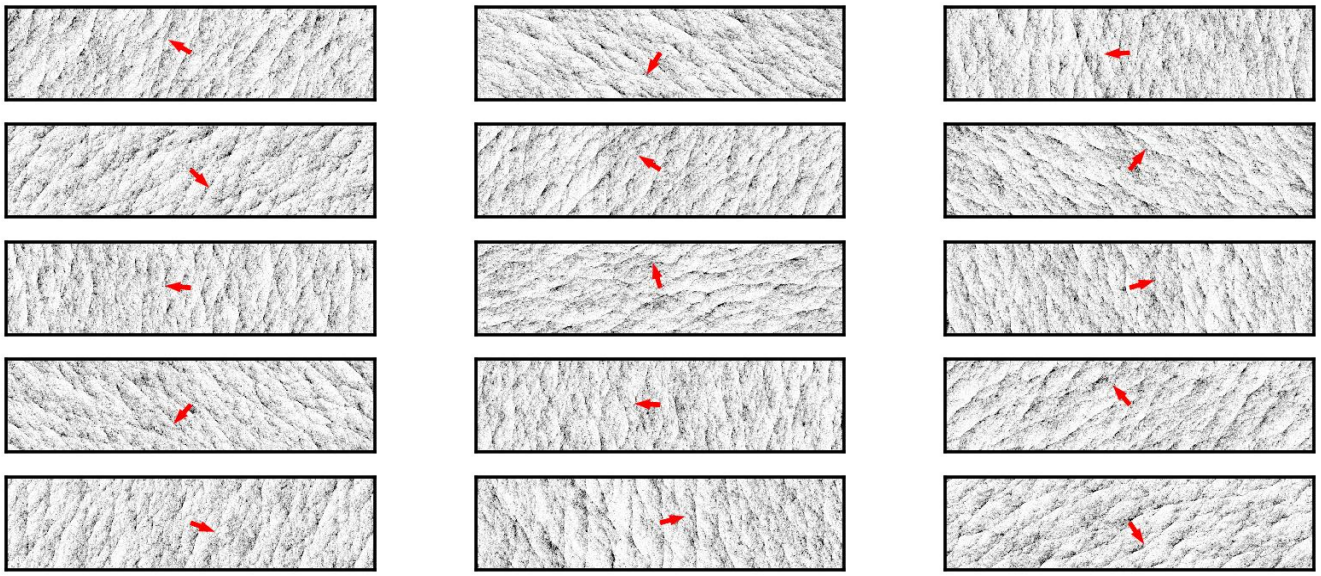

$\eta = 0.30$.

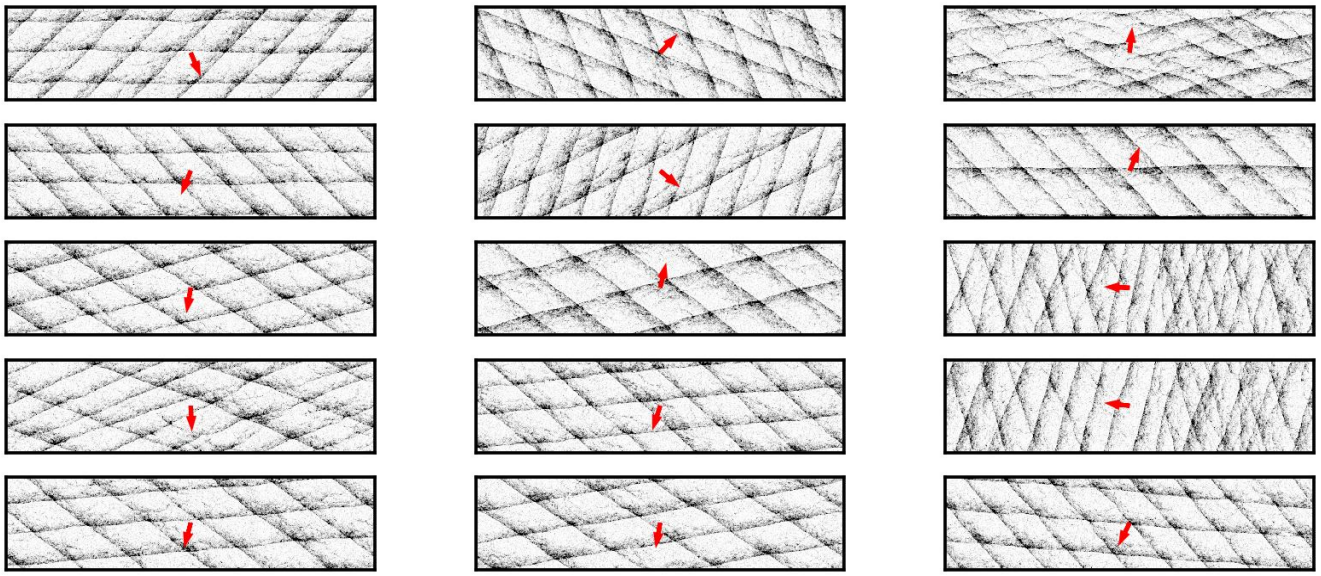

$\eta = 0.35$.

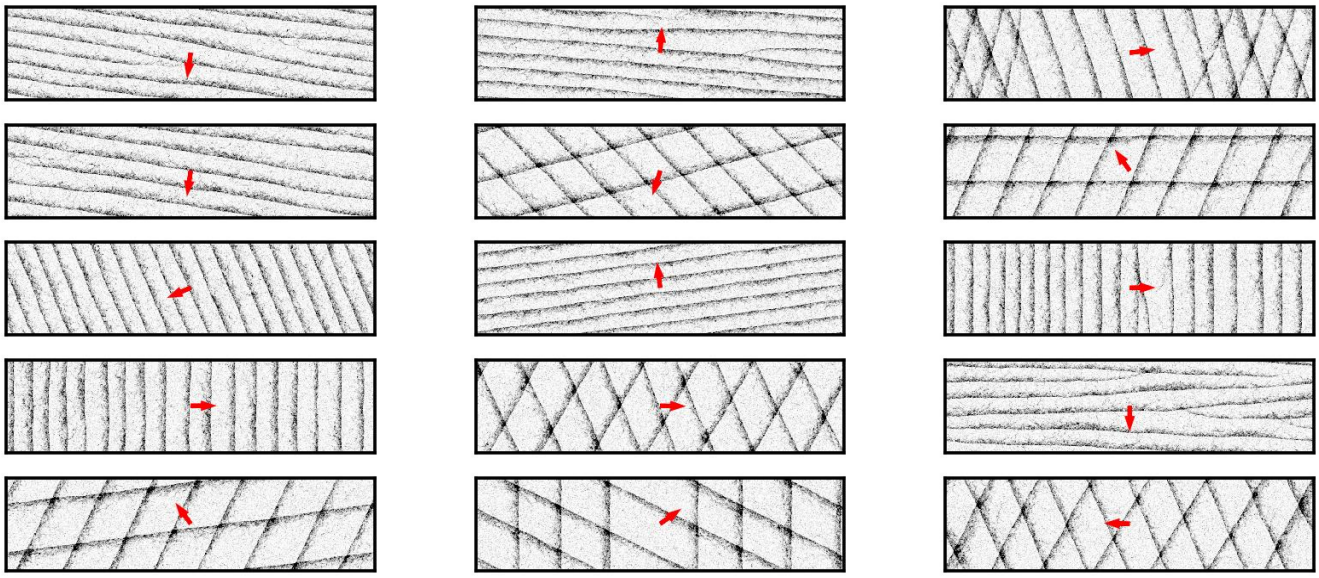

7.3 Aspect Ratio 1 : 16

In this subsection, we present simulation results for the same parameters as in the Letter, but with an aspect ratio of the simulation domain of 1 : 16. That means $L_x = 5013.2$ and $L_y = 313.3$. In the following we present snapshots of 15 realizations after 2×10^5 time steps, started from random initial conditions for $\eta = 0.30$. For this noise strength all realizations are in cross sea state on a quadratic simulation domain of the same area or for an aspect ratio of 1 : 4.

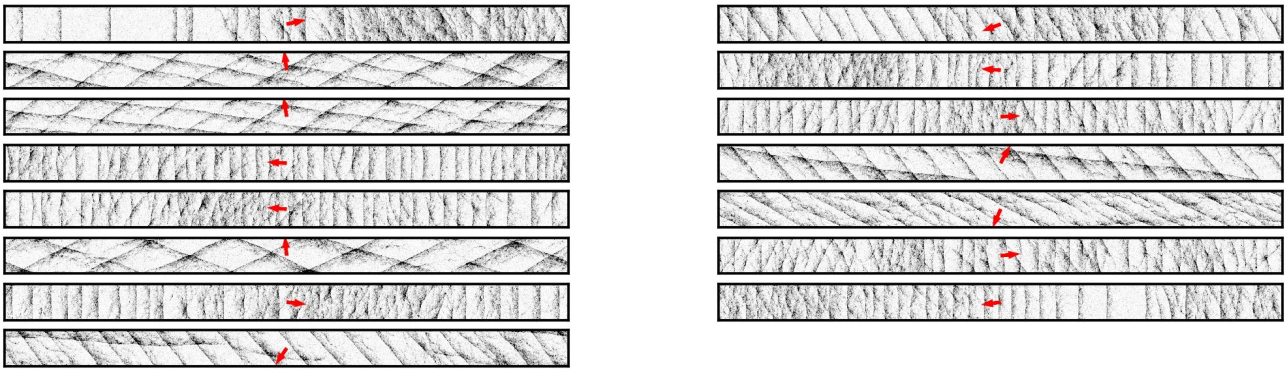

Here, we find only some realizations in cross sea state. These are the realizations that have approximately a vertical average propulsion direction. Realizations with an average velocity in x-direction are not in cross sea state. Furthermore, some of them are not yet forming a regular pattern and possibly much longer simulation times are necessary, see also Sec. 5. It is reasonable that cross sea states are suppressed for average velocity directions along the x-axis because the meshes of the cross sea pattern simply do not fit in the simulation domain (compare the mesh size of those realizations moving in vertical direction). This might be one possible reason why the cross sea state has not been reported before. If one is interested in studying the band state with as many fronts as possible, one might use channel-like simulation domains and initial conditions with velocities along the channel direction. In that case, the cross sea states are suppressed.

Figure S14: Example snapshots for Toner-Tu phase (a) and band phase (b) for simulation domains with aspect ratio of 1 : 16 with $L_x = 5013.2$ and $L_y = 313.3$. Other parameters are as in the Letter. The snapshots were taken after 2×10^5 time steps.

Nevertheless, we still find an overall picture similar to the one we got from quadratic simulation domains.

For small noise strength, the system is in the Toner-Tu phase, see Fig. S14 (a) for an example. For larger noise strengths one finds cross sea or band states, depending on the average direction of propulsion, see above. For larger noise strengths there are only band states, see Fig. S14 (b) for an example, and for even larger noise strength, there is disorder (not shown).

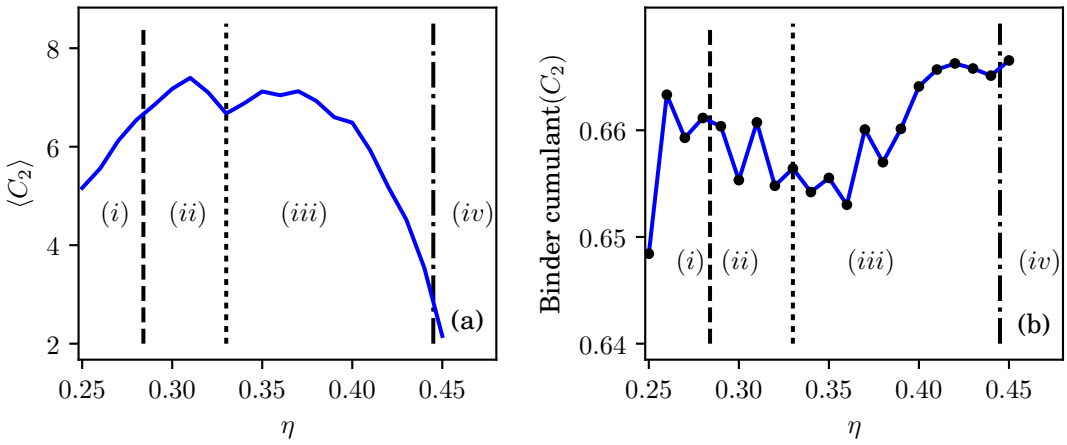

Figure S15: (a) C_2 order parameter and its Binder cumulant (b) for parameters as in the Letter but with an aspect ratio of the simulation box of $1:16$. The vertical lines show the positions of the transitions measured on a square domain.

For completeness, we also show the average value and the Binder cumulant of the C_2 order parameter in Fig. S15. However, for reasons described above, there is not much value in it and it is not possible to clearly identify the transitions. We conclude that for numerical studies of phases of the Vicsek model in the limit $N \to \infty$ it is essential to choose very large simulation domains in both directions L_x and L_y.

7.4 A Smaller Density: $\rho_0 \pi R^2 = 1$

In this subsection we show simulation results for $N = 10^6$ particles, $L = 1772.5$ and $v = R = 1$. Compared to previous simulations, the density is smaller by a factor of two. Here, there is on average one particle within a unit circle. For this parameter set, the system needs more time to reach its steady state. We use a thermalization time of 8×10^5 for $\eta \leq 0.27$ and 4×10^5 for $\eta > 0.27$. The transitions are shifted towards smaller noise, compared to the higher density, as expected. Qualitatively, however, the system behaves equivalently, see Fig. S16 and snapshots below. We estimate the transition (iii) to (iv) roughly from snapshots and the transitions from (i) to (ii) and from (ii) to (iii) from local minima in the Binder cumulant of C_2. Between (ii) and (iii), there seem to be two minima in the Binder cumulant, see Fig. S16 (b). However, there is only one transition. The Binder cumulant fluctuates a lot depending on the number of realizations in cross sea or in band state. With more realizations, these fluctuations should decrease and we expect only one peak between (ii) and (iii).

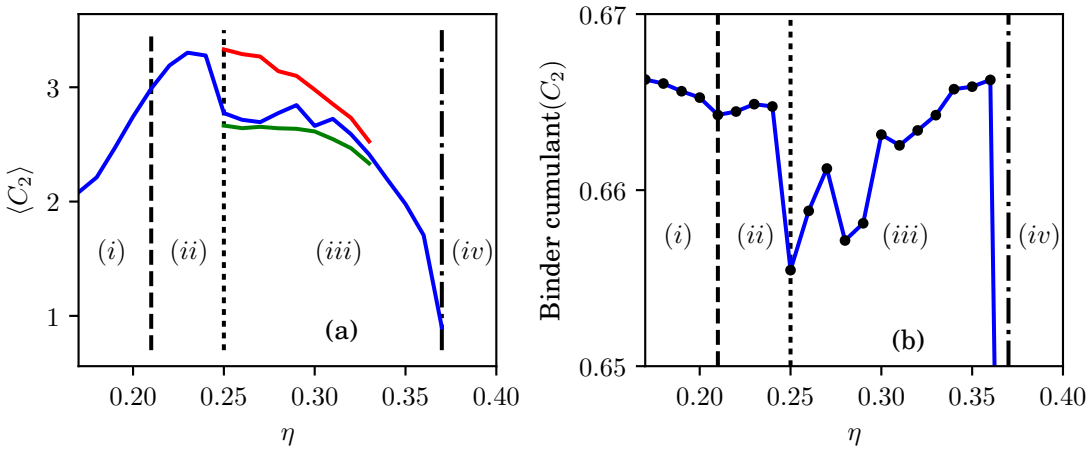

Figure S16: (a) C_2 order parameter and its Binder cumulant (b) for $N = 10^6$, $L = 1772.5$, other parameters are as in the Letter. Averages have been take over 15 realizations and 10^4 time steps after thermalizing for 8×10^5 time steps for $\eta \in [0.17, 0.27]$ and 4×10^5 time steps for $\eta > 0.27$. The red and green line in (a) show averages over only cross sea and only band realizations, respectively.

In the following we show 15 snapshots of the system in the Toner-Tu phase ($\eta = 0.17$):

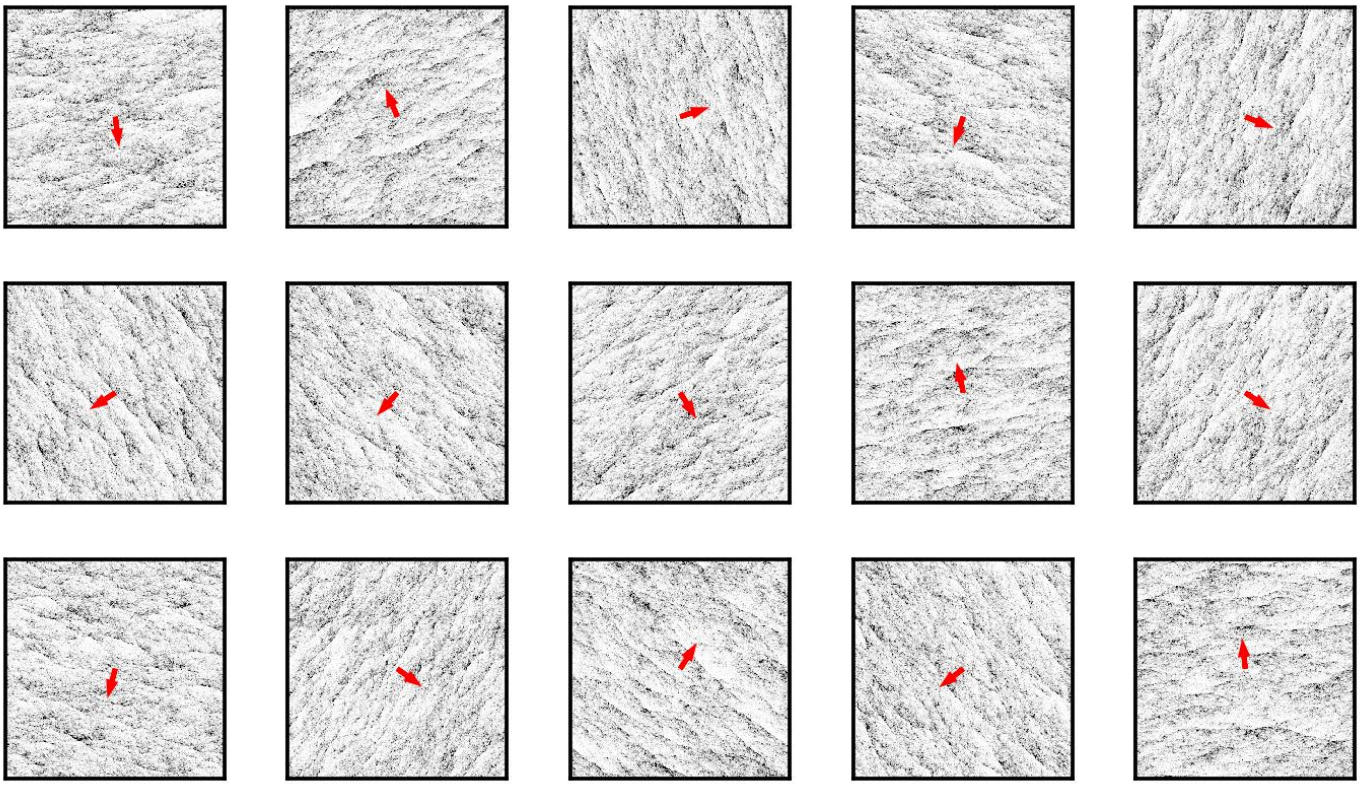

In the cross sea phase ($\eta = 0.24$) we find four of fifteen realizations not perfectly ordered after 8×10^5 time steps. For that reason we simulated a bit longer and show snapshots after 1.2×10^6 time steps. Here, only one realization is not yet regularly ordered (first realization in second row):

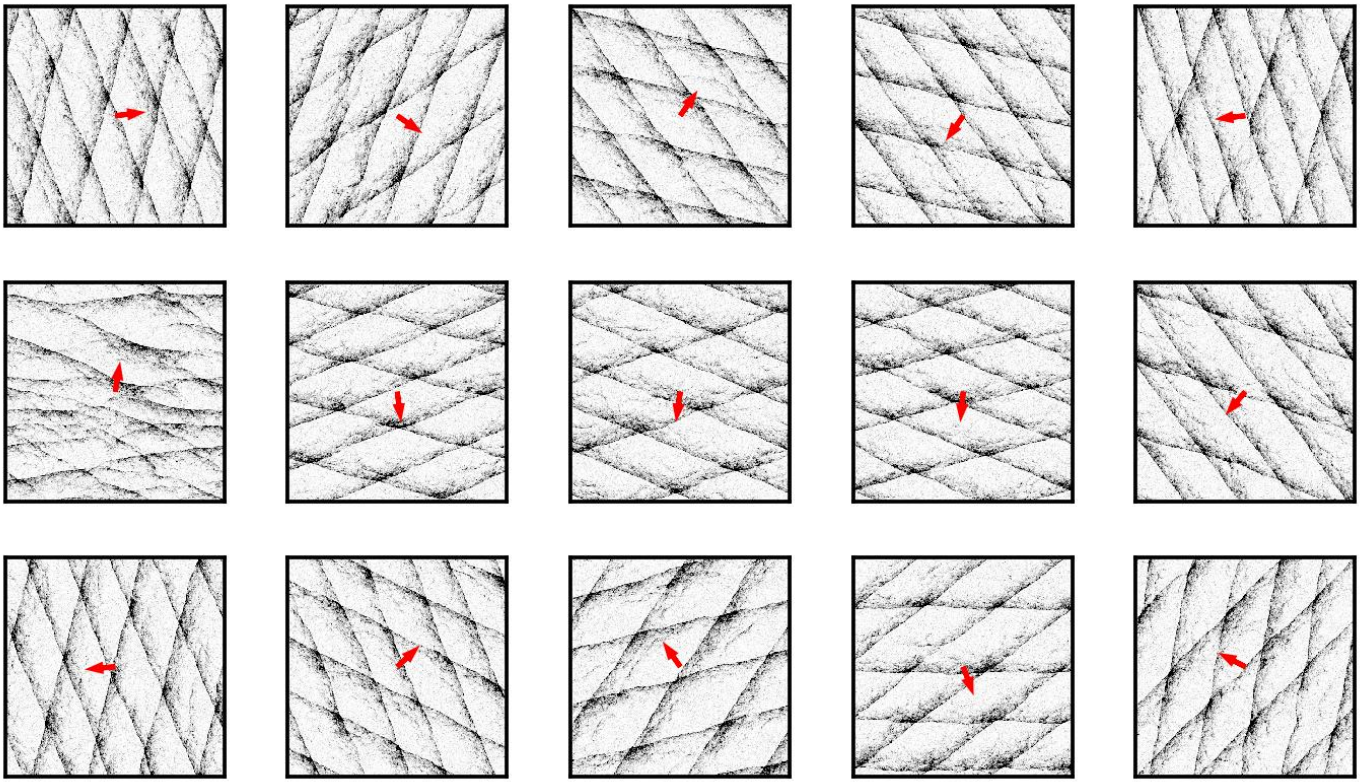

And for $\eta = 0.29$ with some realizations in band state and some in cross sea state:

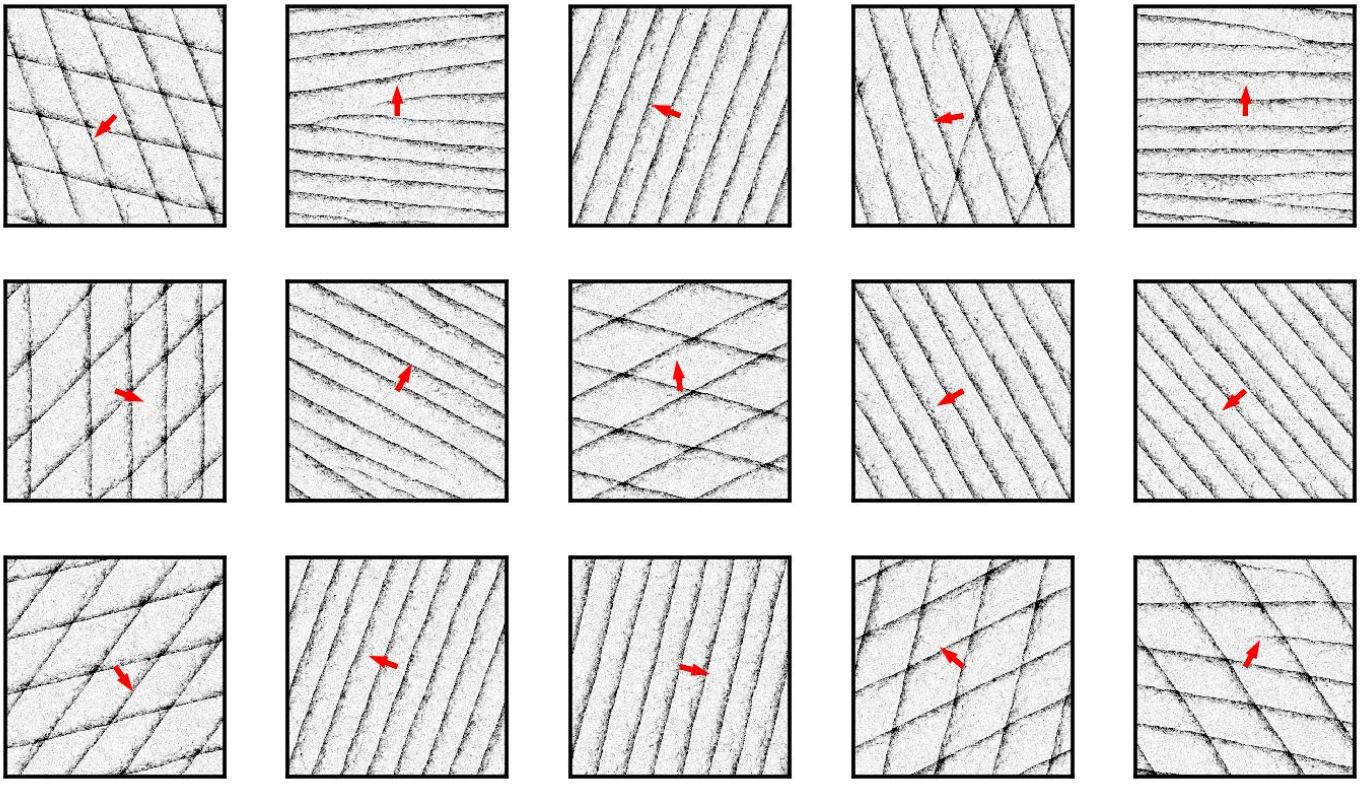

8 Initial Conditions

We used random initial conditions for all simulations presented in this work. That means all particles have been placed independently of each other at uniformly distributed random positions within the simulation box and with a random orientation also drawn uniformly from the interval $[0, 2\pi]$. Such disordered initial conditions appeared to us as the most reasonable ones. However, we have also tried to initialize the particles still at uniformly distributed random positions but all with the same initial orientation. In that case, we observe that the polar order gets lost first and then builds up again with a new random orientation. Thus, such homogeneous polar ordered initial conditions seem to lead to very similar results.